UNIVERSITY OF CALIFORNIA
RIVERSIDE

Lateral Snow Transport, Fire and Changing Treelines in Mount San Gorgonio, California, U.S.A.

A Thesis submitted in partial satisfaction
of the requirements for the degree of

Master of Science

in

Geological Sciences

by

Charles Dustin Burton

September 2012

Thesis Committee:
Dr. Richard A. Minnich, Chairperson
Dr. Mary L. Droser
Dr. Michael F. Allen

The Thesis of Charles Dustin Burton is approved by:

_____

_____

_____

Committee Chairperson

University of California, Riverside

ACKNOWLEDGEMENTS

Foremost, I am exceptionally fortunate to have been provided this opportunity by my wife, Dawn Burton. She paid the bills and did the care taking of our home and kids while I was studying at UCR, in the field for research or on Geology field trips with the GCEC crew. The results of which were two wonderful daughters, Sierra and Cambria, and a warm home to return to from my duties and excursions. Very closely behind my wife, I am extremely grateful to my advisor, Richard A. Minnich, for providing me with this research opportunity. His help in formulating ideas for this research and his wealth of knowledge and prior work on the local area were instrumental to this final product. I couldn't have done this without his years of study in the local San Gorgonio Mountains which laid the foundation and underlying knowledge for my research work and my ability to further the understanding of the treeline forest of Mt. San Gorgonio. I am also thankful to Mary L. Droser and Michael F. Allen for their support and interest in my thesis as members of my committee. Their help and evaluation have helped make my thesis exemplary. Additional thanks to my GCEC/UCR compadres; specifically Dr. Martin Kennedy, Baird King, Darryl Kohut, Michael Trumbower, Cassy Meyers, and Brett Goforth for memorable adventures (the 2009 GCEC trip and Baird's Field Work), good times and great feedback. Thanks also to Dr. Kennedy for the funding provided for my field work as well as his ability to peak my initial interest and assist in getting me in the GCEC program.

DEDICATION

I dedicate this work to my daughters Sierra Bryce Burton and Cambria Juniper Burton. If nothing else, I hope my efforts, the knowledge I've gained and my passion for learning will inspire similar passions within their lives. Specifically a love for learning, a passion for science, a desire for self-improvement and a wanting for the outdoors.

ABSTRACT OF THE THESIS

Lateral Snow Transport, Fire and Changing Treelines in Mount San Gorgonio, California, U.S.A.

by

Charles Dustin Burton

Masters of Science, Graduate Program Geological Sciences
University of California, Riverside, September 2012
Dr. Richard A. Minnich, Chairperson

The mountain tree line correlates with the limit of carbon gain in photosynthesis, a temperature dependent process linked to atmospheric lapse rates. Studies of tree lines often do not focus on specific mechanisms that limit their distributions, including lateral snow transport (LST) and snow drifting, as well as wildfires. At Mount San Gorgonio (elevation 3505 m) in the eastern San Bernardino Mountains, 130 km east of Los Angeles, the subalpine forest tree-line (*Pinus flexilis, P. contorta*) has been stable over the 20th century. Above 3000 m blowing snow and snow drifting associated with the jet stream, combined with topographic wind enhancement, including forests denuded by fires, can significantly affect timberline dynamics. The reduction of surface roughness due to tree removal accelerates LST and lowers the timberline on leeward slopes subject to increased snow deposition. This paper evaluates LST at three ridgeline timberline sites in the San Gorgonio Wilderness that were burned in 1863, 1869 and 1951. Post-fire tree

growth response is measured by using 200 m long sampling quadrats that traversed from windward to leeward slopes. Metrics include tree cover, height and diameter data. The results indicate that the LST is enhanced by fire which increases wind speeds, windward slope snow ablation, and leeward slope snow deposition, slowing tree establishment and growth. In the krummholz zone near San Gorgonio summit, recurrent damage from wind, snow and ice produce shear injury to windward slope tree canopies downwind (northeastward), result in continuous LST. On leeward slopes, late summer or perennial snow cover, maintains bare zones (tree lines) due to tree mortality, the snow decrease the growing season and increase the probability of tree death. At global scales, the tree line is predicted to ascend mountain slopes with planetary warming because the upper elevation boundary of woody vegetation is assumed to represent temperature limitations to positive net photosynthesis. An essential issue in the growth of plant canopy is the separation of intrinsic productivity from physical dieback over ecological time scales: What is carbon gain in canopy versus the rate of canopy removal due to wind-driven disturbances and snow burial over the life of the tree that reduces photosynthetic capacities? Without mass loss from LST, a hypothetical increase in forest canopy would permit tree colonization to higher elevations than the modern empirical limit. These findings are applicable to other mountain ranges at temperate latitudes subject to jet stream induced LST, and must be accounted for in the observation and prediction of tree lines in response to global climate change.

Table of Contents

List of Figures

List of Tables

List of Appendices

INTRODUCTION

One of the most eye-catching vegetation boundaries in global biogeography is the mountain tree line, which correlates with the limit of carbon gain in photosynthesis, a temperature dependent process linked to atmospheric lapse rates (Tranquillini 1979; Grace et al 2002). Studies of tree lines often do not focus on specific mechanisms that limit their distributions (Smith et al. 2003; Johnson et al. 2004). One process is lateral snow transport (LST). In temperate and polar latitudes, mountain tree lines extend into the tropospheric jet stream, and storm winds phased with precipitation frequently exceed hurricane force speeds. Jet stream winds, accelerated by Venturi and Bernoulli forces over mountain barriers, and solid precipitation produces "blowing snow." Snow lifted from the snow surfaces in concurrence with ambient buoyant snowflakes with large surface to volume ratios advect laterally across topographic surfaces. The LST process creates snow drifting, i.e., the heterogeneous distribution of accumulated snow as a result of wind and precipitation in ambient flow interacting with the snow surface over topography, the blowing snow moving by saltation similar to barchan dunes (Lehning et al. 2008). Snow forms aeolian drifts, ridgeline cornices, and gallery accumulations in leeward terrain such as cirque headwalls, nivation hollows and avalanche chutes under wind deceleration and gravity. While having the appearance of avalanches, accumulations on steep leeward catchments represent the continuous process of blowing snow. Forests just below the tree line ameliorate blowing snow by locally increasing atmospheric friction, reducing ground wind speeds and snow accumulation heterogeneities due to air friction.

LST is not only a primary factor in tree lines over ecological time scales, but also has profound influence on glacial geomorphology at Quaternary time scales. Heterogeneous snow accumulation affects cirque aspect asymmetry, i.e., steep headwalls (maximum snow accumulation and plucking from LST) on leeward exposures, and conversely on windward snow ablation zones (Gilbert 1904), and engender favored orientations of glaciers (Evans 2006; Mindrescu 2010). Modern perennial snow patches can be viewed as transitional forms to glaciers because their mass balance properties are similar to that of glaciers (Watanabe 1988). Indeed, late snow fields occupy favorable accumulation zones in cirques suggest that modern LST processes occurred at greater magnitudes in full glacial climates.

In southern California LST across mountain crests is unidirectional toward the northeast due to southwesterly winds of waves in the Polar Front jet stream coinciding with cold fronts, and precipitation (Minnich, 1984; Owen et al. 2003). Nearly all winter precipitation above 3000 m is snow (Minnich 1986) and the interannual distribution of snow drifts is fixed with respect to snow ablation on windward slopes and snow accumulations on leeward slopes, with largest accumulations intermittently forming perennial snow in years with above normal precipitation. LST is enhanced by wildfires which remove forest and accelerate surface winds. In California, mediterranean climate characterized by protracted summer drought, tree lines are influenced by wildfires which produce temporary tree lines, and episodes of post-fire LST. Snow drifting constrains post-fire tree establishment compared to topographically sheltered forests.

This study examines the interaction between LST, tree line and wildfires on Mt. San Gorgonio in the San Bernardino Mountains of southern California, 130 km east of Los Angeles. While krummholz trees grow to the summit (elev. 3500 m; Minnich 1984), tree limits form distinct topographic boundaries in which krummholz forest on windward slopes gives place to barrens on leeward slopes. We evaluate LST on forest successions at three fire sites and at the tree line on the summit of San Gorgonio. Our objective is to evaluate how LST: (1) controls modern tree line distribution, (2) affects fire succession at the tree line, and (3) whether recent climate change has increased the altitude of the tree line.

Study Area

The San Gorgonio Mountain area (Figure 1) is a series of east-to-west trending ridges that include San Gorgonio Summit (3500 m), San Bernardino Ridge (3200 m), and the Ten Thousand Foot Ridge (3000 m). Bedrock is mostly Mesozoic granite (SCAMP: http://geomaps.wr.usgs.gov/archive/scamp/html/index.html). The north and northeast exposures have small glacial cirques with moraines dating to the last glacial maximum (20-16 ka, Owen et al. 2003). These have steep headwalls which grade down slope into talus derived from avalanche chutes between intermittent bedrock outcrops. Unglaciated exposures have uniform slopes of 20 to 30º, with small nivation hollows with steep fluvial debris cones on north to northeast facing exposures.

The climate is mediterranean with winter precipitation from cyclonic storms of the jet stream. Summers are dry except for occasional thunderstorms of the North American monsoon. Mean annual precipitation ranges from 75-100 cm, with amounts

exceeding 200 cm in the wettest years. The vegetation consists of subalpine forest dominated by *Pinus contorta* (lodgepole pine) and *P. flexilis* (limber pine), with scattered shrub understory of *Chrysolepis sempervirens, Arctostaphylos patula*, and *Ceanothus cordulatis*. Pine stands below 3200 m consist of medium poles 10-20 m height. Above 3100 m forests gradually develop krummholz physiognomy with greater crown spread than height of low, twisted trees flagged mostly SW to NE, with tree stature decreasing to 1 m tall cushions on the most wind-exposed ridges.

METHODS

The database was developed from field samples, Google Earth imagery, aerial photographs, historical records and previous studies (Minnich 1984, Owen et al. 2003).

Fire History

Stand replacement fires (Figure 1) were mapped from aerial photographs taken in 1938 and 1952, as well as ground photographs taken between 1863 and 1910 (online; USC Digital Library, Los Angeles Public Library). The year of fire was determined from newspaper accounts. The burns consisted of discrete areas of dead forest or post-fire patches of even-sized young trees. The 1869 burn at Jackstraw (JST) was described "at the head of the Santa Ana River" in the Los Angeles Star on July 17 and September 11.

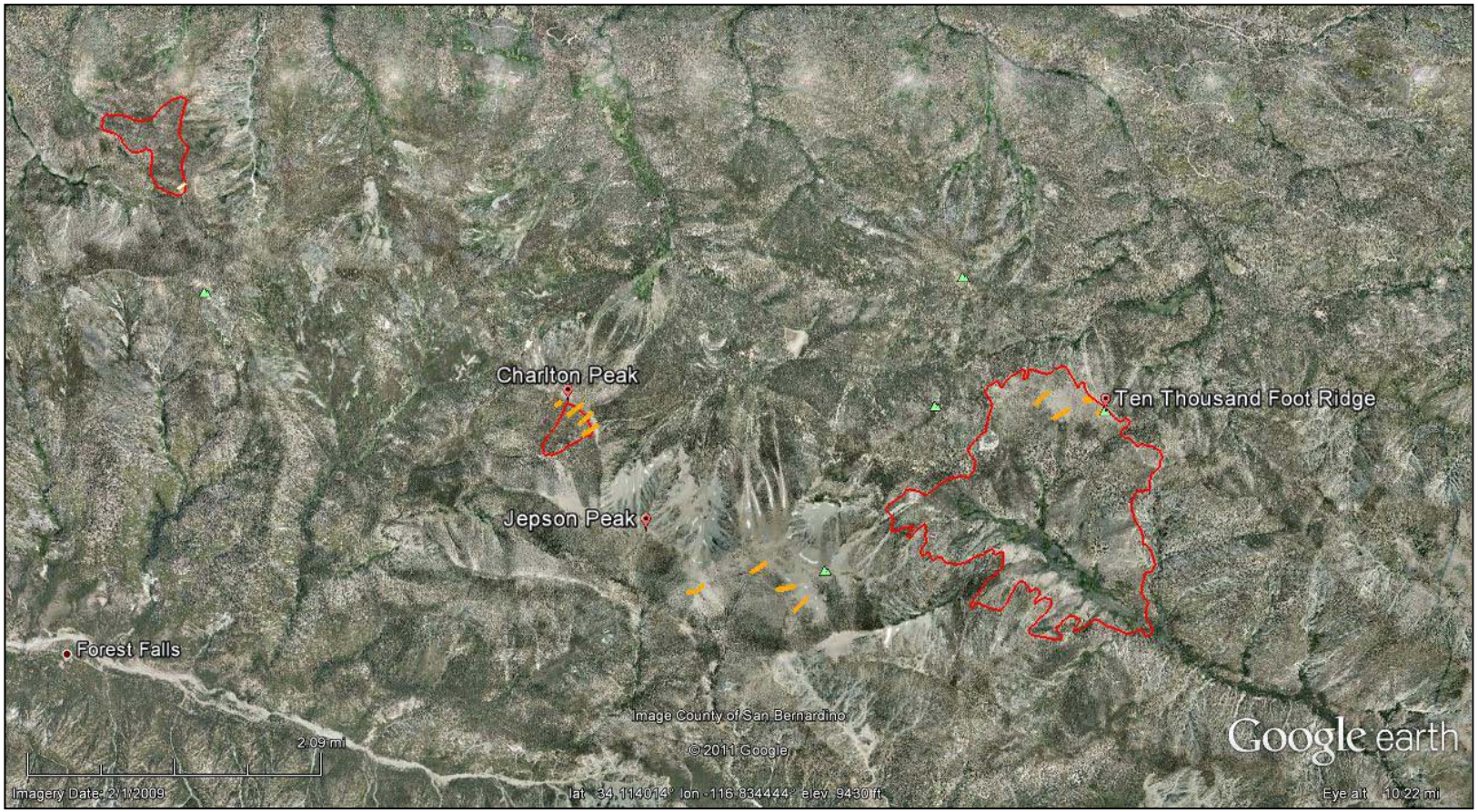

Figure 1: Google Earth Image of Mt. San Gorgonio field sites; Jackstraw (JST), Charlton Peak (CHP), San Gorgonio (SGR), and Ten Thousand Foot Ridge (TFR) (from east to west). Orange rectangular shaped outlines are sample quadrats. Fire perimeters are shown in red.

The 1863 burn at Charlton Peak (CHP) was recorded in a ground photograph taken by Lukens in 1900 (Lukens Box 7, Album 5, The Huntington Library, San Marino California), and was not evident in a photograph taken from San Bernardino in April 1863. The period 1862-64 was one of the most extreme droughts in California history (Minnich 2008). The 1951 burn at Ten Thousand Foot Ridge (TFR) is documented in US Forest Service records. This stand-replacement burn was remapped for accuracy using 1952 aerial photographs in Earth Explorer (US Geological Survey, http://edcsns17.cr.usgs.gov/NewEarthExplorer/). These burned areas were all mapped onto Google Earth and transferred to basemaps using ARC GIS.

Perennial Snow Years

Years with perennial snow on Mount San Gorgonio were reconstructed from newspaper accounts beginning in 1878 in the *Los Angeles Times* and other local newspapers. Observations of such a remote area are remarkably complete because late summer/fall snow cover on the highest peaks in southern California was a novelty to residents living in a hot summer climate in the Los Angeles coastal plains and interior valleys. Beginning in 1969 perennial snow was mapped using field and aerial photographs (Minnich 1984; Owen et al. 2003). Years with perennial snow were correlated with total annual precipitation at Los Angeles.

Sample sites

The sample sites are San Gorgonio Summit (SGR), Charleton Peak (CHP, 3.2 km NW of SGR), Ten Thousand Foot Ridge (TFR, 3.4 km NE of SGR), and Jackstraw (JST,

10 km W of SGR). Each site has four quadrats except for JST, an area without LST, which has only one quadrat. Quadrats are 20 m X 200 m or 40 m X 100 m (Figure 1). Quadrats traversed from southwest facing windward slopes and over ridgelines to northeast facing leeward slopes. The quadrats traverse slopes ranging from 16.7 to 42.7%, with elevations ranging from 2,985 to 3,473 m.

Methods

Quadrat borders were first established in the lab using Google Earth imagery and topographical maps of the region. Elevations were determined with the Google Earth elevation cursor and contour lines on US Geological Topographic Sheets (San Gorgonio Mountain quadrangle). Vertical profile views and built in compass features on Google Earth were used to ensure that quadrats were designed to transition from SW windward slopes to NE leeward slopes. The high resolution aerial images provided information on tree cover to obtain best sampling strategy and aided in locating start points in the field. Fire perimeter outlines were superimposed on Google Earth to ensure sample sites where within fire boundaries.

Quadrats were drawn with the "add polygon and ruler" feature on Google Earth to ensure accurate length, width and bearing in ˚T. Quadrat printouts, with GPS and bearing information, and a handheld GPS were used to find the starting point for each quadrat in the field. Once determined, start points were marked with a rebar stake. Reel tape was laid out to the pre-determined length using the magnetic compass and pre-determined bearings. From this centerline, 10 m tape and the magnetic compass were used to create

perpendicular right and left borders from the reel tape. Flagging tape and flags were used to mark the measured borders.

Each field measurement began at the quadrats start point and finished at its endpoint. Elevation profiles recorded quadrat topography from start to finish at 10 m intervals. The handheld GPS provided latitude, longitude and elevation readings for each interval and the magnetic compass determined slope aspect for each interval. A line intercept plot was performed over the plot centerline to obtain a measure of species and their density within the plot by measuring the length of tape each individual occupied. Trees (living and dead) were all referenced within the quadrat on a local x-y axis coordinate system. The reel tape determined each individuals distance from the start point and the 10 m tape determined their distance right or left from the centerline.

Tree diameter at breast height (dbh) was measured at ca. 1.5 m with a diameter tape. For irregularly shaped individuals a homogeneous diameter was picked to measure dbh. Tree heights within arm reach (< 2.3 m) were measured with a tape, and the taller trees (> 2.3 m) were measured with a clinometer. A distance of 4-10 m (depending on tree height) away from the tree was measured by tape and the angle to the trees top and base were measured with the clinometer. The tree height was determined by multiplying the final angle (top + or – base) times the distance from the tree. Species was identified from needle counts. Dead trees were classified as downed (logs) or standing (snags). At TFR the most recent burn with numerous downed logs, a magnetic compass was used to determine the bearing of downed trees from the root axis to the tree top. Notes were made

for individuals with unique characteristics like those associated with high winds or snow burial (i.e. heavily browned needles, desiccated branches, and curved stems). The measurements were taken during 17 days in the field in the summer and fall of 2010 and encompassed 13 quadrats, an area of 48,200 m^2 and over 2000 trees.

Field log entries were transcribed into Microsoft Excel to sort and manipulate data into visual representations of field conditions to show and analyze forest trends. Tree size measurements were broken into six size categories at 1.0 m intervals for tree height and 5 cm intervals for dbh. Trees were further grouped into 10 m intervals beginning from the starting point of each quadrat in order to observe demographic changes in relation to topography. Scatter plot regressions compare windward versus leeward tree heights and tree diameters with respect to distance from the ridgeline. Tree cover data was derived from line intercept data taken in the field and from Google Earth tree cover plots. Logs were grouped by compass bearing.

Long-term population characteristics were made at SGR by georeferencing aerial photographs taken in 1938 and 2009. Individual trees in both aerial photograph baselines were georeferenced based on unique local nearest-neighbor configurations. We counted the number of trees in common to both coverages, “recruitment” (new trees in 2009), and mortality (trees disappearing after 1938). Cover was estimated using a random point matrix in a gridden transparency overlay.

RESULTS

Lateral Snow Transport

U.S. National Weather Service radiosonde data at San Diego and precipitation data for Los Angeles show that winter storms consistently produce high winds at 700 mbar, a standard pressure level which normally lies just below the altitude of Mount San Gorgonio (Minnich 1984, 1986). Ambient velocities range from 12-25 m s^{-1}, rarely 35 ms-1, and increase with precipitation amount (Figure 2A). Surface winds on the mountain are likely greater than ambient due to Venturi and Bernoulli acceleration over physiographic barriers in stable (nonconvective) air, characteristic of cold fronts in California (Minnich 1984).

LST results in spatially fixed interannual winter snow free zones (accumulation deficit / total precipitation) and late summer snow fields (accumulation surplus / total precipitation), although with interannual changes in the time of melt as a function of total snowfall. About 80% of the mean annual precipitation correlates with 700 mbar wind directions between 220 - 250 º accounts for >80% of total annual precipitation (Figure2B; from Minnich 1984). As a consequence, LST advection and surface snow transport is from southwest to northeast across the mountain (Figure 2B; Minnich 1984; Owen et al., 2003). Late summer or perennial snow is found on the northeast side of ridgelines, and leeward slope catchments including cirque headwalls (Figure 3). LST snowfields become conspicuous only after upslope terminal zonal snowmelt ascends to the highest

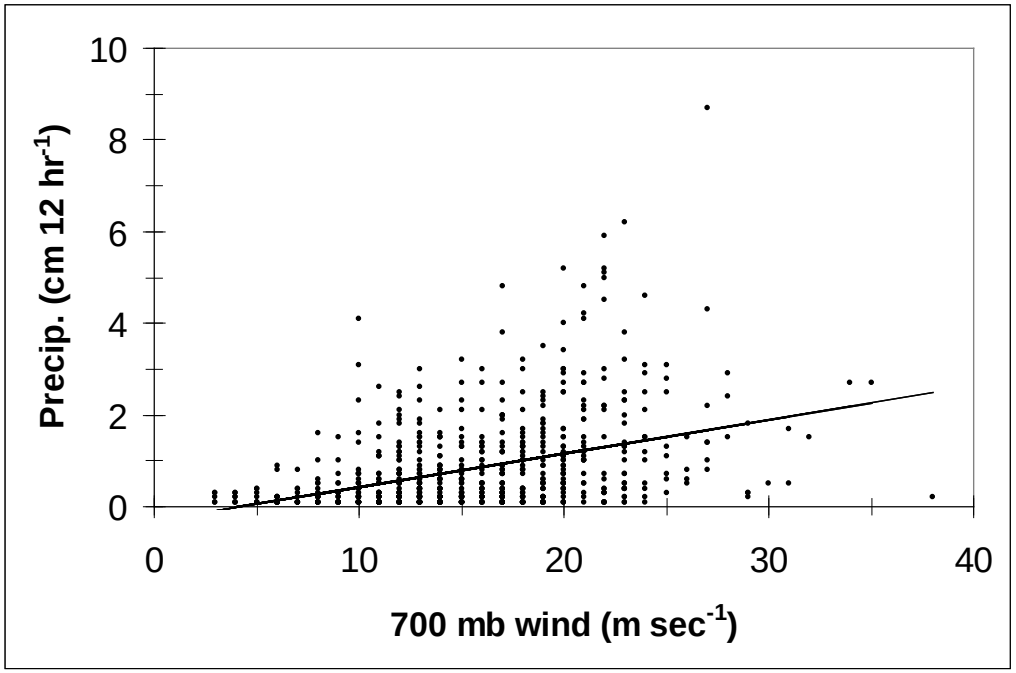

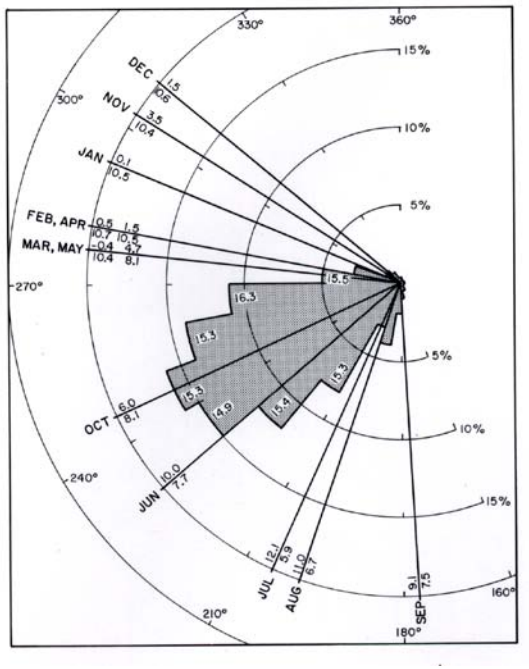

Figure 2A (left): Precipitation amount (cm 12 hr^{-1}) versus wind velocity at 700-mbar (m sec^{-1}, data from Minnich (1986)). **Figure 2B (right):** 700-mb (ca. 3100 m) climatic data and precipitation rose for the San Diego radiosonde (1956 to 1980). Prevailing wind axis for each month is shown with mean 700-mb temperature (top numeral), wind velocity (bottom numeral). Percent of total precipitation by wind direction (10 deg interval) is shown with respective mean storm wind velocities (source: National Oceanic and Atmospheric Administration, 1956-1980).

peaks, usually in June and July. Snow melt precedes the zonal snowline in krummholz zones on southwest facing exposures, and the most wind-exposed ridgelines were free of snow in winter (Minnich 1984). Snow cornices also developed in stand-replacement burns at CHP and TFR (Figure 3).

Perennial snow has been reported on San Gorgonio in 30% of years since 1878. Historical newspapers recorded perennial snowfields in most years with > 50 cm annual precipitation at Los Angeles (> 125% percent of normal, PON). All years with > 60 cm correlated with perennial snow (Table 1; Appendix 2). Most snowfields survived only one summer but the largest patches persisted as long as four years when the 3-5 year moving average precipitation exceeded 50 cm, including 1905-07, 1914-17, 1937-41, 1978-81, and 1992-95 (Figure 4). Newspapers suggest that snow drifts persisted nearly a decade in the late 19th century (1884-1893) as a consequence of two winters with >220% PON (1883-84, 1889-90). These winters each produced snow accumulations surviving melt for years, even through intervening normal to dry winters. In a recent case, abnormally large perennial snow fields in 1993 survived the relatively dry winter of 1993-94 before enlarging again in the wet winter of 1994-95 (Figure 3). In normal and below normal years the last snow disappears from May to August.

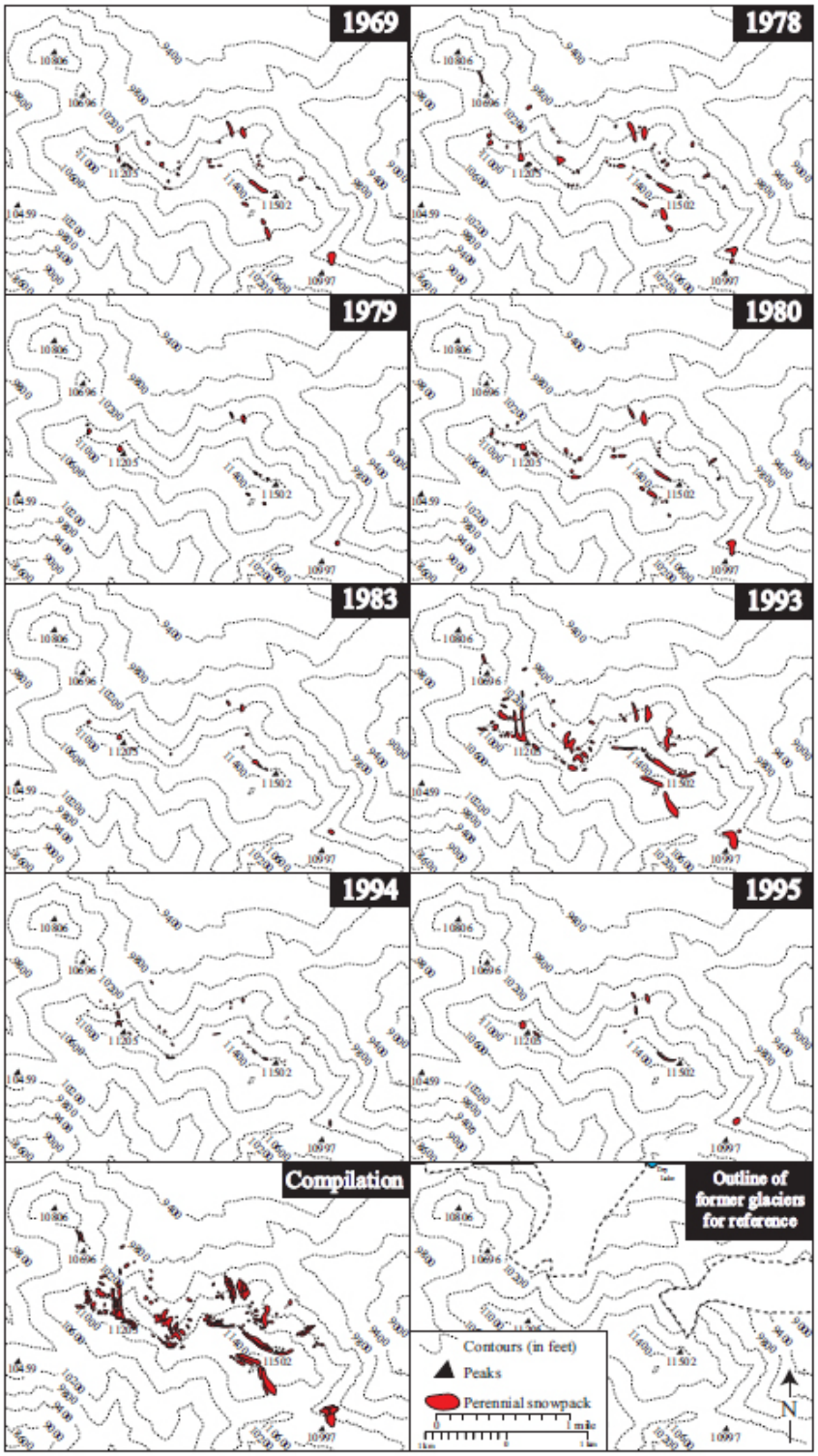

Figure 3: Perennial snow patches on San Gorgonio Mountain for 1969-1995. (Repository of the journal, *Geology*)

Table 1. Total annual precipitation at Los Angeles Downtown and frequency of perennial snow years (average annual precipitation 37.5 cm).

Precipitation, Los Angeles (cm)	Freq. years	Years, perennial snow	Percent
< 30	48	2	4.2
30-40	31	4	12.9
40-50	23	11	47.8
50-60	11	10	90.9
60-70	7	7	100.0
>70	7	7	100.0

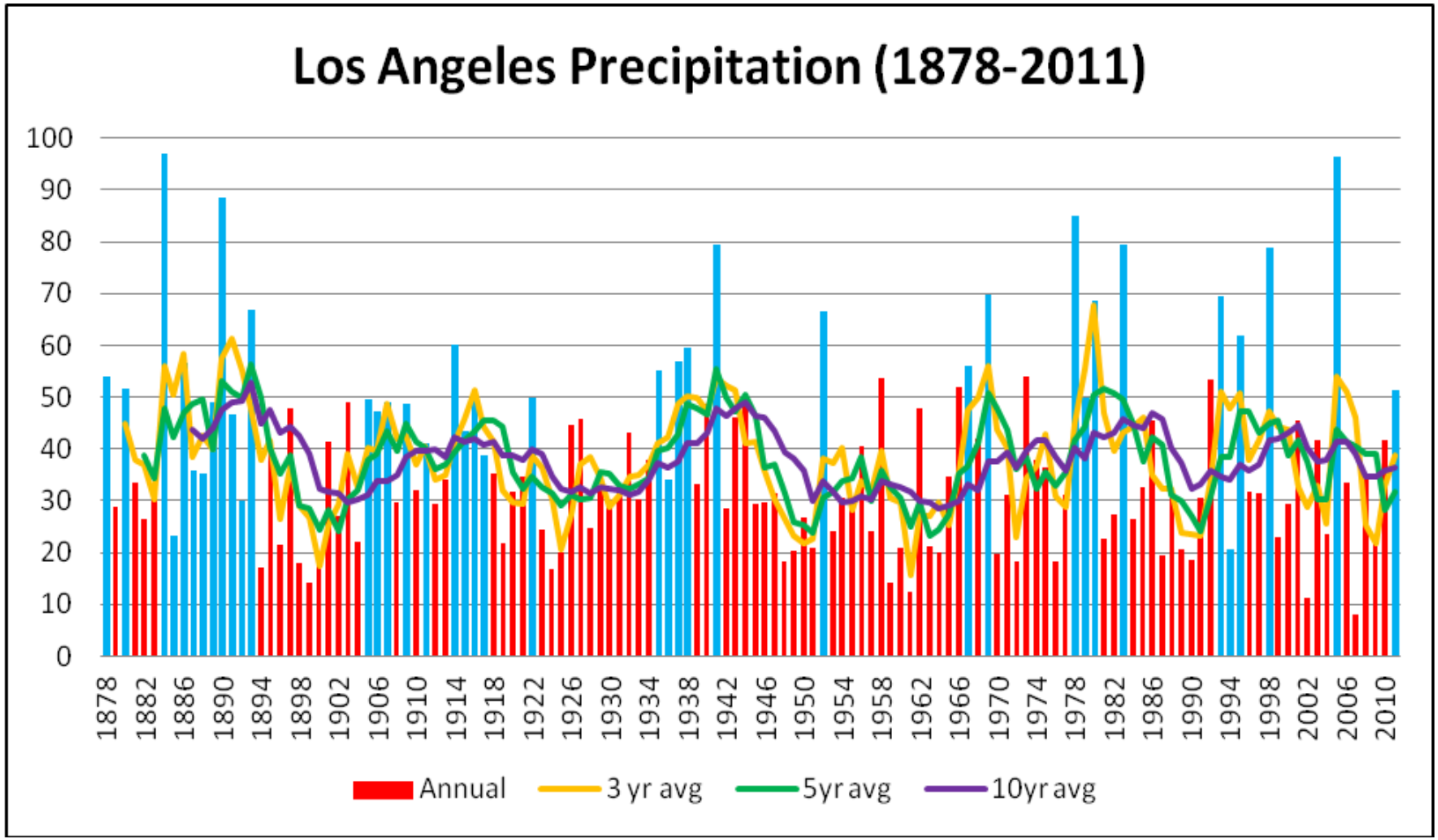

Figure 4: Precipitation data at Los Angeles Downtown for 1878 to 2011 (July to June). X-axis is precipitation in cm. Blue bars indicate perennial snow on Mount San Gorgonio.

Post-fire succession in lateral snow transport

Tall subalpine forest covers most of the region but becomes increasingly stunted toward ridgelines. In krummholz zones there are abrupt transitions from low forest on southwest facing to barrens on northeast facing leeward slopes, the boundaries invariably following ridgelines. Barrens continue downslope and become extensive, especially on the headwalls of glacial cirques.

Similar abrupt transitions occur in stand-replacement burns (whole-stand mortality) characteristic of California subalpine forest (Figure 5). Thin-barked lodgepole and limber pine seldom survive surface or crown fires due to fatal cambial damage, leaving masses of standing dead trees (Minnich 1988; Minnich 2007, Fites-Kaufman 2007). Since both pines have nonserotinous cones (seed is fire-killed), the recolonization of burns is dependent on wind dispersed seed from adjacent unburned forest.

The pace of post-fire succession decreases with altitude. The greatest rate of vertical growth, as expressed in ratios of tree stature versus dbh occurred at JST and TFR at 3000 m, but decreases with altitude at CHP (3200 m) and SGR (3400 m, Figure 6). The JST site, which lies in the wake of the San Bernardino Ridge to the southwest, illustrates typical post-fire succession of subalpine forest, in this case 142 years after fire. The forest consists of 40% cover of pole size trees as tall as 10 m (Figure 7A; Table 2). Aerial photographs show that recruits in the burn have smaller crown head diameters than trees in surrounding unburned forest. The wide range in stem dbh from 0 to 40 cm indicates the development of uneven-aged stands from continuous recruitment.

Figure 5: Windward (snow ablation) to leeward (snow deposition) transitions from the top counter clockwise: **a.** Mt. San Gorgoni. **b.** Charlton Peak (7/24/2010). **c.** Ten Thousand Foot Ridge (6/30/2010).

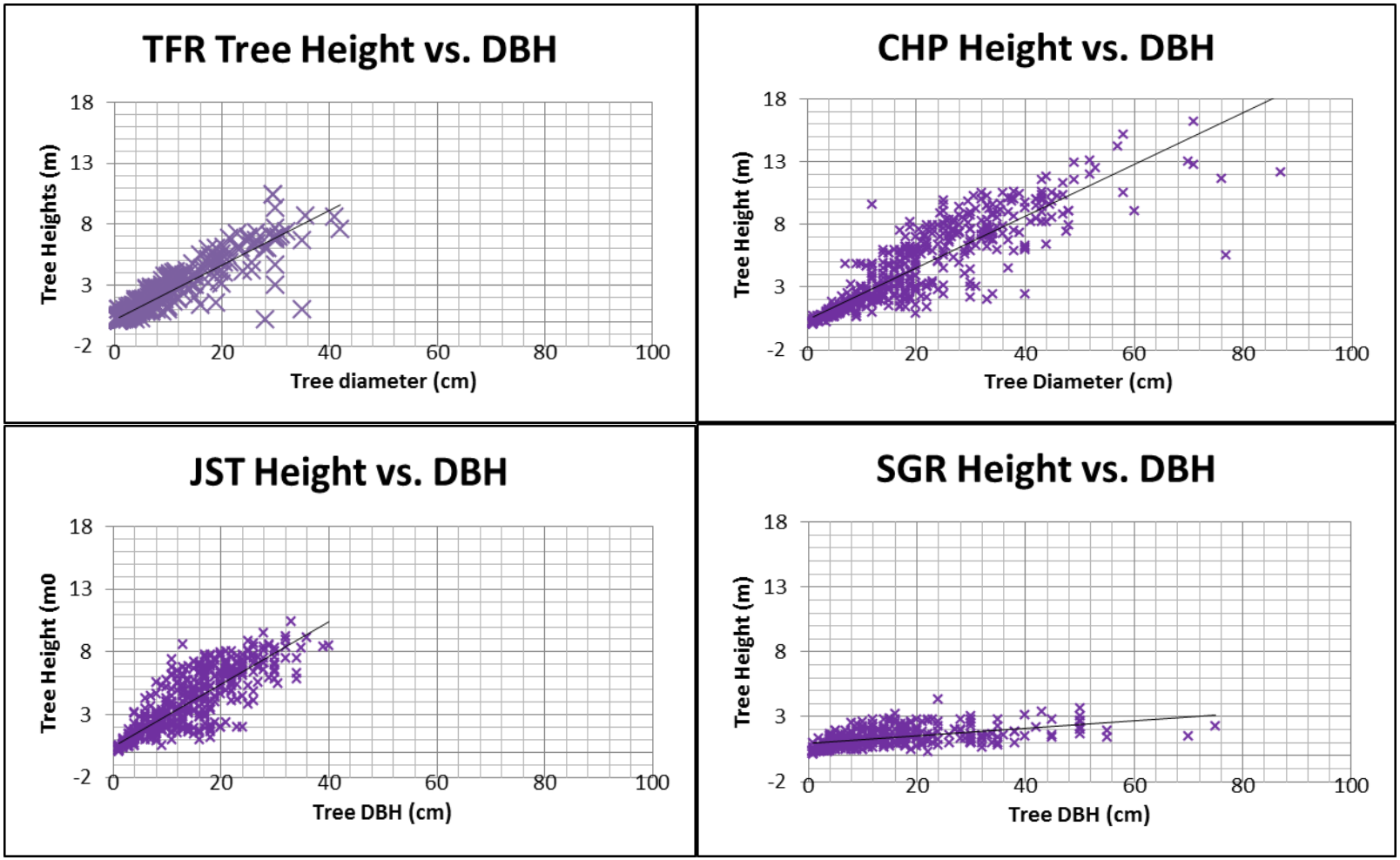

Figure 6: Regressions of diameter at breast height (dbh) versus tree height. Jackstraw (JST), Ten Thousand Foot Ridge (TFR), Charlton Peak (CHP) and San Gorgonio Summit (SGR).

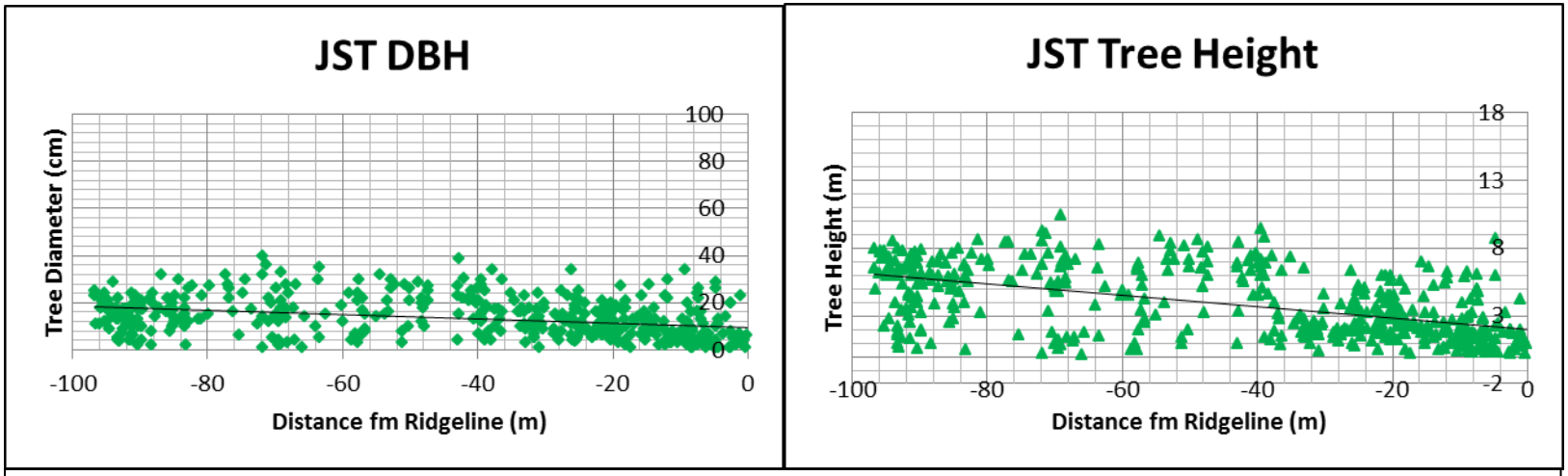

Figure 7: Tree diameter (cm) and height (m): A. Jackstraw (JST). B. Charlton Peak (CHP). C. Ten Thousand Foot Ridge (TFR). D. Mt. San Gorgonio (MSG). The zero point along transects is the ridgeline dividing windward and leeward slopes. Negative numbers indicate windward distance, and positive numbers leeward distance from the ridgeline. Windward and leeward slopes were not distinguished at JST.

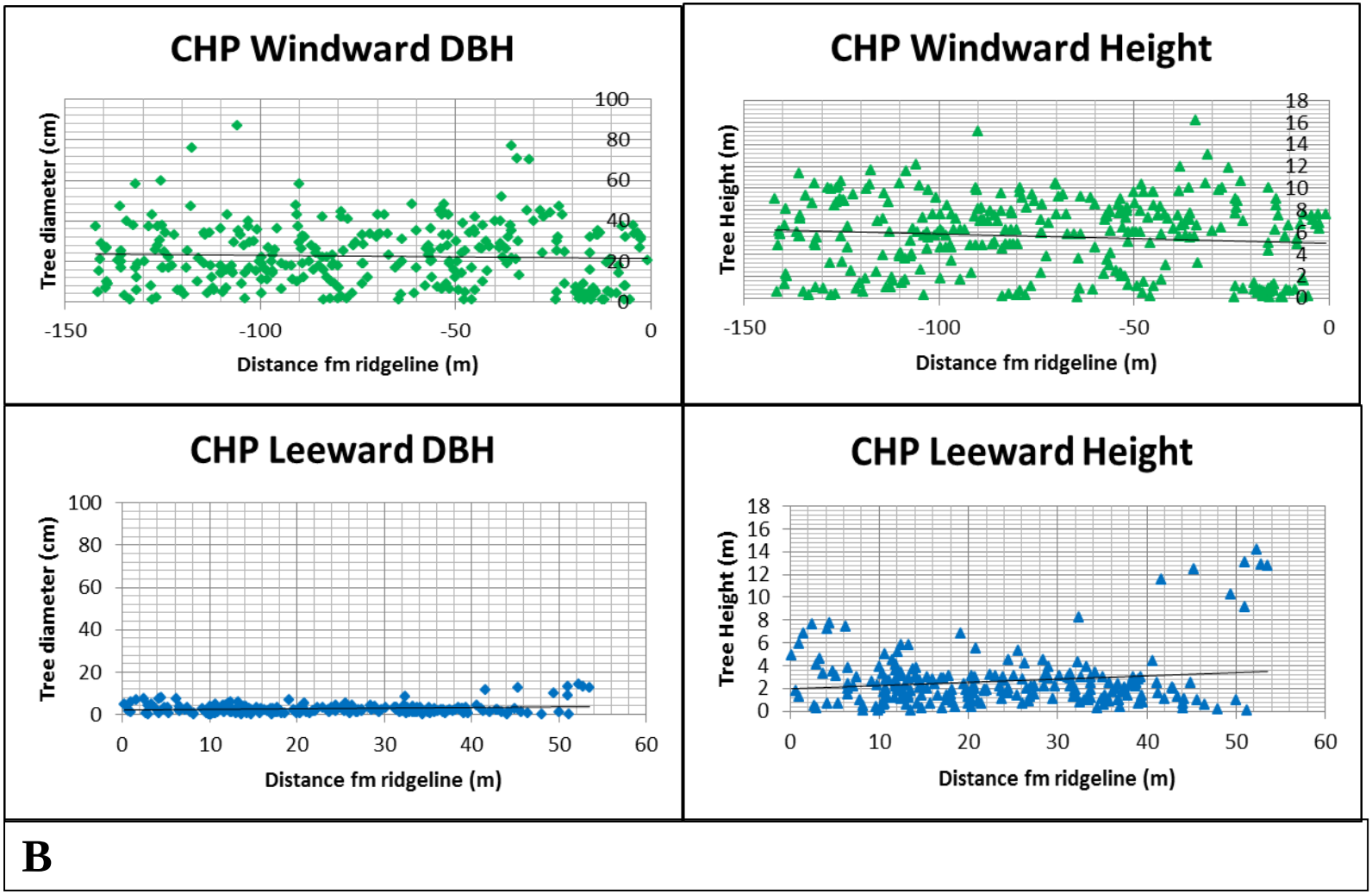
CHP Windward DBH
Tree diameter (cm)
100
80
60
40
20
0
-150
-100
-50
0
Distance fm ridgeline (m)
CHP Windward Height
Tree Height (m)
18
16
14
12
10
8
6
4
2
0
-150
-100
-50
0
Distance fm ridgeline (m)
CHP Leeward DBH
Tree diameter (cm)
100
80
60
40
20
0
0
10
20
30
40
50
60
Distance fm ridgeline (m)
CHP Leeward Height
Tree Height (m)
18
16
14
12
10
8
6
4
2
0
0
10
20
30
40
50
60
Distance fm ridgeline (m)

B

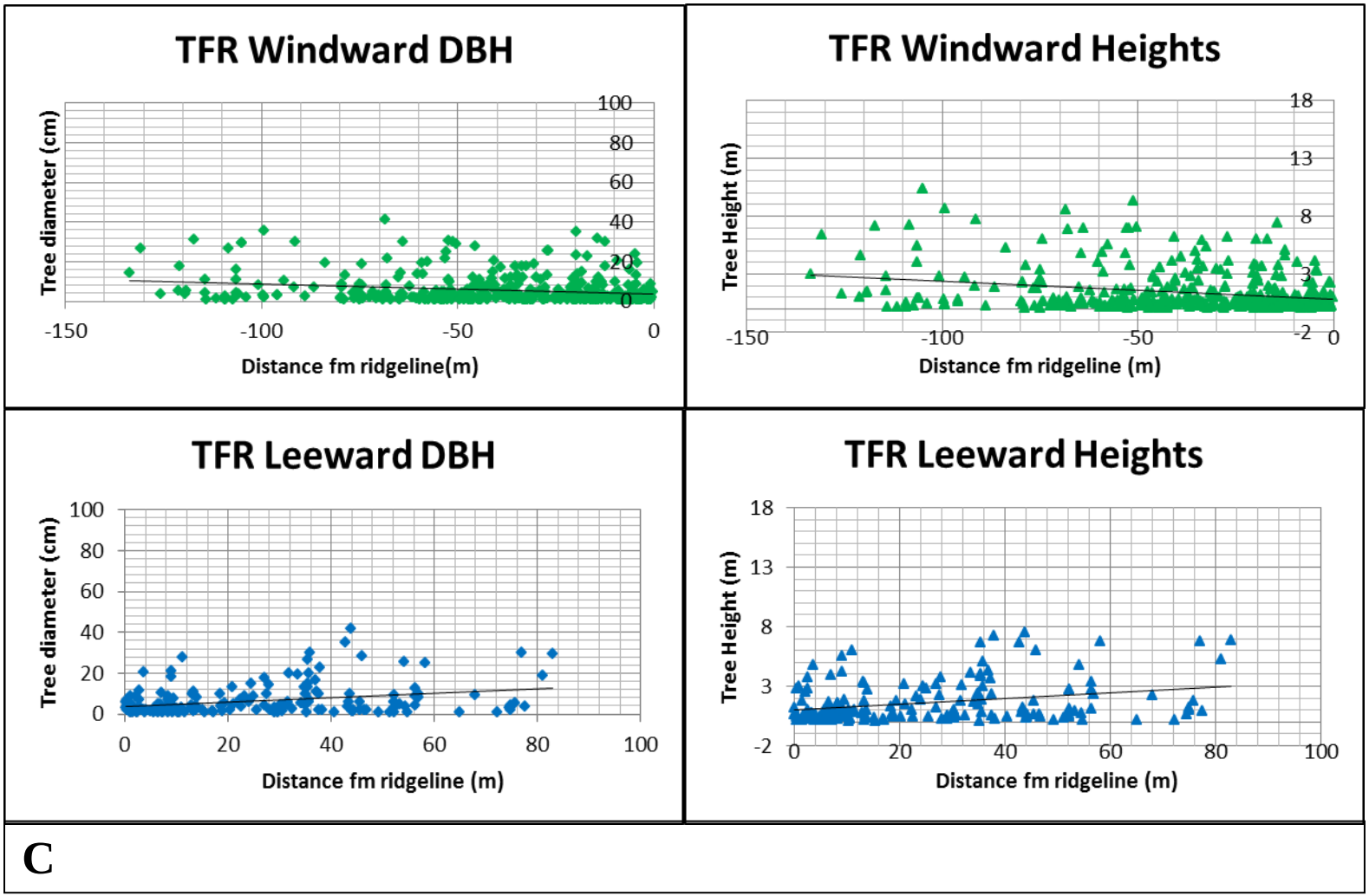
TFR Windward DBH
Tree diameter (cm)
100
80
60
40
20
0
-150
-100
-50
0
Distance fm ridgeline(m)
TFR Windward Heights
Tree Height (m)
18
13
8
3
-2
-150
-100
-50
0
Distance fm ridgeline (m)
TFR Leeward DBH
Tree diameter (cm)
100
80
60
40
20
0
0
20
40
60
80
100
Distance fm ridgeline (m)
TFR Leeward Heights
Tree Height (m)
18
13
8
3
-2
0
20
40
60
80
100
Distance fm ridgeline (m)
C

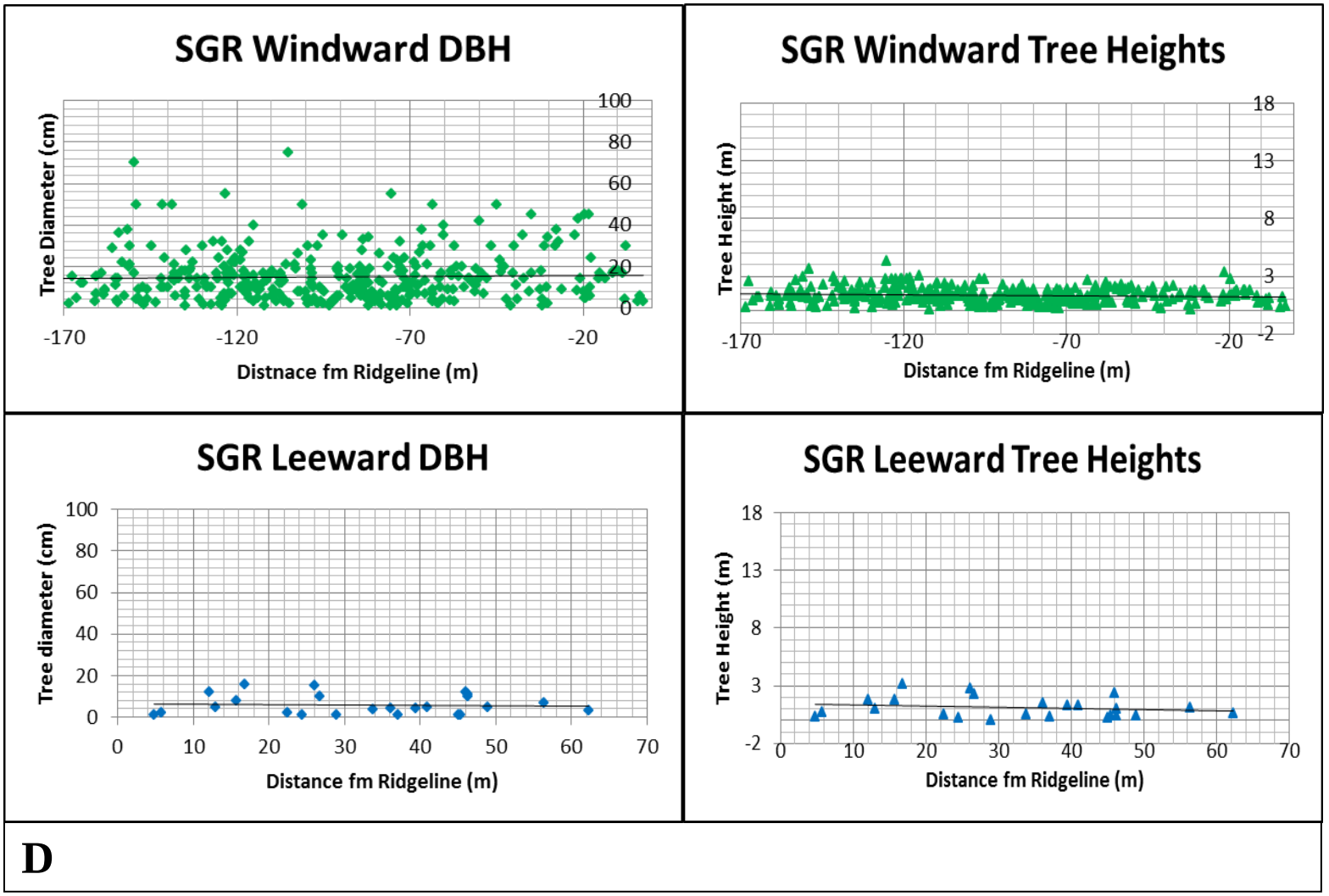
SGR Windward DBH
Tree Diameter (cm)
100
80
60
40
20
0
-170
-120
-70
-20
Distnace fm Ridgeline (m)
SGR Windward Tree Heights
Tree Height (m)
18
13
8
3
-2
-170
-120
-70
-20
Distance fm Ridgeline (m)
SGR Leeward DBH
Tree diameter (cm)
100
80
60
40
20
0
0
10
20
30
40
50
60
70
Distance fm Ridgeline (m)
SGR Leeward Tree Heights
Tree Height (m)
18
13
8
3
-2
0
10
20
30
40
50
60
70
Distance fm Ridgeline (m)

D

Table 2 Tree cover and density at Charlton Peak, Jackstraw and Ten Thousand Foot Ridge (source: Google Earth).

	Site	Elev. (m)	Exposure	Total Trees 2011	Tree Cover % 2011
Charlton Peak	CHP-W-1	3170	SW	42	17
	CHP-W-2	3205	SW	41	20
	CHP-W-3	3225	S	62	22
	CHP-W-4	3196	SW	39	21
	CHP-W-5	3227	SW	31	19
	CHP-L-1	3224	NE	7	4
	CHP-L-2	3258	NE	67	16
Jackstraw	JST-L-1	3003	NE	144	48
	JST-L-2	3028	NE	138	42
	JST-L-3	3040	NE	199	40
Ten Thousand Foot Ridge	TFR-W-1	3038	SW	36	18
	TFR-W-2	3005	SW	24	26
	TFR-W-3	2992	SW	29	24
	TFR-W-4	2957	W	42	12
	TFR-W-5	2992	W	23	10
	TFR-W-6	3043	W	35	15
	TFR-L-1	2984	NE	22	1
	TFR-L-2	2988	NE	34	1
	TFR-L-3	2998	NE	16	3
	TFR-L-4	3069	N	40	4

Trees exhibit uniform size and diameter distributions within the 1869 burn, but discontinuously form abrupt shifts to large trees with greater canopy diameters outside the fire boundary. Stem densities estimated from Google Earth imagery range from 576 to 796 stems ha^{-1}, with tree cover ranging from 40 to 48% (Table 2).

The CHP site, only 200 m higher in elevation, has limited forest cover and stature over a comparable period of 147 years since fire (Figure 7B). The windward slope had few shrubs and trees in a ground photograph taken in 1900, and in aerial photographs in 1938 (Figure 8). Present-day trees have comparable diameter and height distributions as JST, but most stems are mostly 4-8 m tall. Rare 16 m tall stems survived the 1863 burn, as evidenced by basal fire scars. The leeward slope has a large bare zone bounded by young trees with dbh < 10 cm and heights < 4 m. These trees established into formerly larger leeward bare zone observed on 1938 aerial photographs. Perennial snow patches are recorded at this site by aerial and ground photographs in 1938, 1978, 1993, and 2005 and snow persisted into September in 1979, 1980, 1983, and 1998 (Minnich 1984, Owen et al. 2003). Tree densities at CHP average 206 stems ha^{-1}, ranging from 28-268 stems ha^{-1} (Table 2) and tree cover ranges from 4 - 22%.

The TFR site has experienced LST since the 1951 fire (Figure 9). Until recently this burn was called the "toothpick" forest on US Forest Service maps in reference to the standing forest of dead trees. Most have since sustained windfall, mostly from SW to NE from root to tree top, apparently in response to storm winds (Figure 10). This relatively young burn has comparable forest succession as CHP (Figure 7C). While tree heights

reach 8 m, most stems are < 3 m. Stem dbh are rarely > 20 cm. There are fewer trees on leeward slopes than windward slopes, mostly with dbh < 20 cm and heights < 3 cm. Small bare zones still exist in areas occupied by midsummer snow cornices, but perennial snow has not been recorded at the site (Figure 3). The abundance of small stems indicates an accelerating rate of recruitment on both windward and leeward slopes. Tree densities average 120 stems ha^{-1}, and cover 24.9% (Table 2**).**

SGR is exposed to the most extreme weather conditions with elevations exceeding 3324 m and unobstructed exposure to ambient winds. There are no records of fire at this site. Windward krummholz trees are almost entirely < 3 m, but stem dbh range to as high as 60 cm, greater than at JST and CHP (Figure 7D**).** Few stems have colonized leeward slopes subject to perennial snow. Population changes of krummholz trees obtained from georeferenced 1938 and 2009 aerial photographs (Figure 11) show that > 90% of stems were recorded in both photograph coverages (Table 3). Assuming linear turnover rates, the mortality rate of only 12.4 stems of 302 stems present ha^{-1} in 1938 implies tree longevity of 1775 years for the whole population. The higher recruitment rate of 67.6 stems ha^{-1}, or ca. 1.0 stems yr^{-1} ha^{-1} implies that stand densities would double only after ca. 300 years.

Field photographs by RAM document widespread canopy damage in windward krummholz of SGR in 1971 and 72 (Figure 12; Minnich 1984). Virtually all trees on San Gorgonio sustained foliar damage that “streamlined” trees on their windward southwest faces, i.e., with little damage in the canopy interior, as well as in leeward canopy. On

windward canopy faces, stem leaders within the upper canopy sustained foliar damage in the upper 1-2 years of branch whorls. Vertical leader emerging above the canopy line sustained dieback of 5-10 years of branch whorls. Windward foliar damage was also recorded on a Google Earth scene on July 17, 2011 having a similar distribution as the 1971-72 event, with injury focused on southwest facing crowns of trees growing on southwest facing slopes.

Georeferenced time-series aerial photographs from 1938 and 2009 document ca. 90% of windward stems are common to both baselines (Table 3). Tree densities in windward zones increased from 75 to 88 stems ha^{-1} since 1938. Forest cover increased from 7.2 to 7.7%. On leeward slopes, trees were buried in snow well into the growing season. The primary tree bole and branches were fatally injured, with surviving canopy limited to basal stems. Many trees perished. Leeward tree death or dieback was phased with late summer and perennial snow after the severe winter of 1969 as well as in 1978-1980 (Minnich 1984). Georeferenced imagery show little evidence of tree invasion into bare zones.

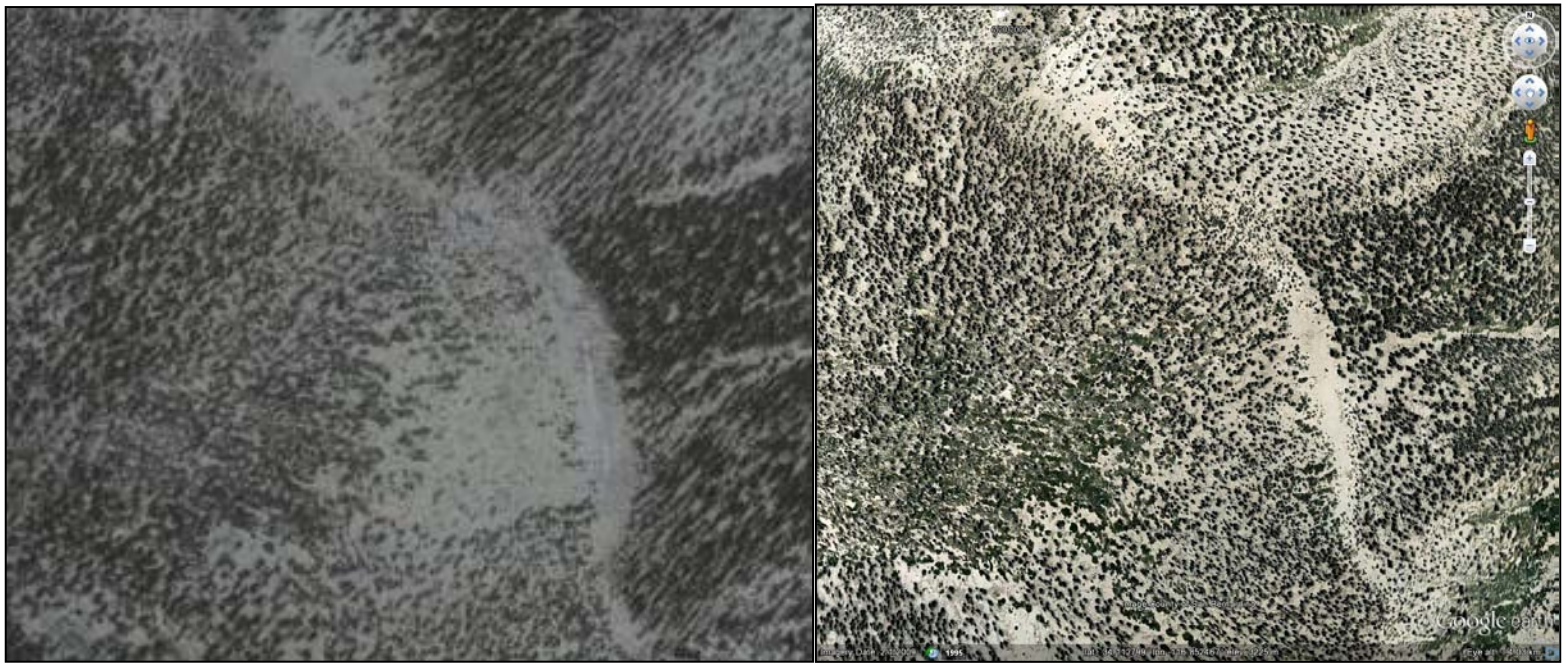

Figure 8: Aerial photographs of Charlton Peak in October 1938 (left) and September 2011 (right). Note the colonization of the burn and snow cornice in the leeward bare zone in 1938.

Figure 9: Oblique aerial photograph of the 1951 Ten Thousand Foot ridge burn after the severe winter of 1980. Note the abundance of standing dead trees, cornices on ridgelines, and small pines emerging above the snow on the windward slope.

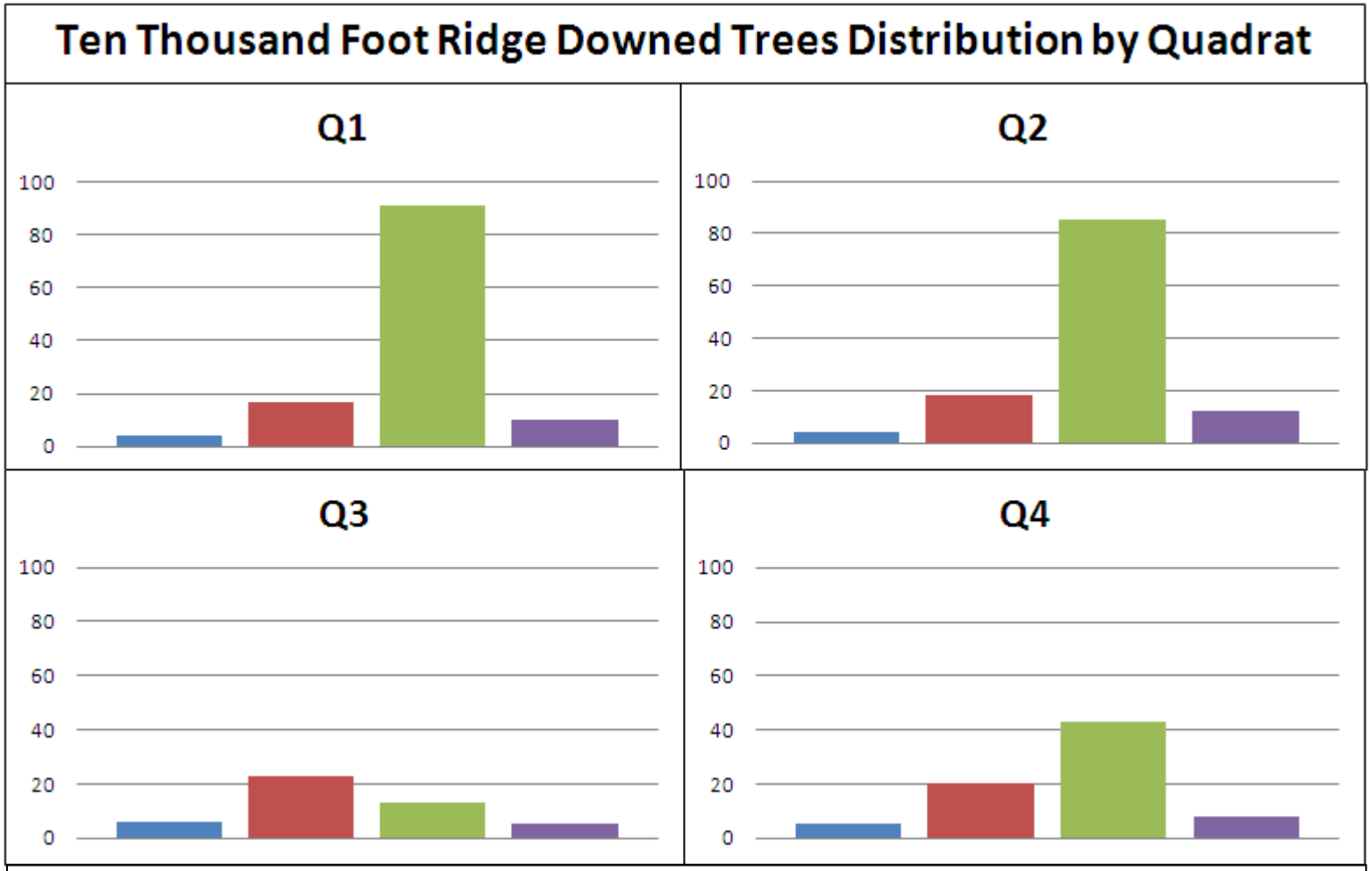

Figure 10: Direction of tree falls in quadrants at four quadrats at TFR. X-axis is frequency. Blue is northeast, red is southeast, green is southwest and purple is northwest.

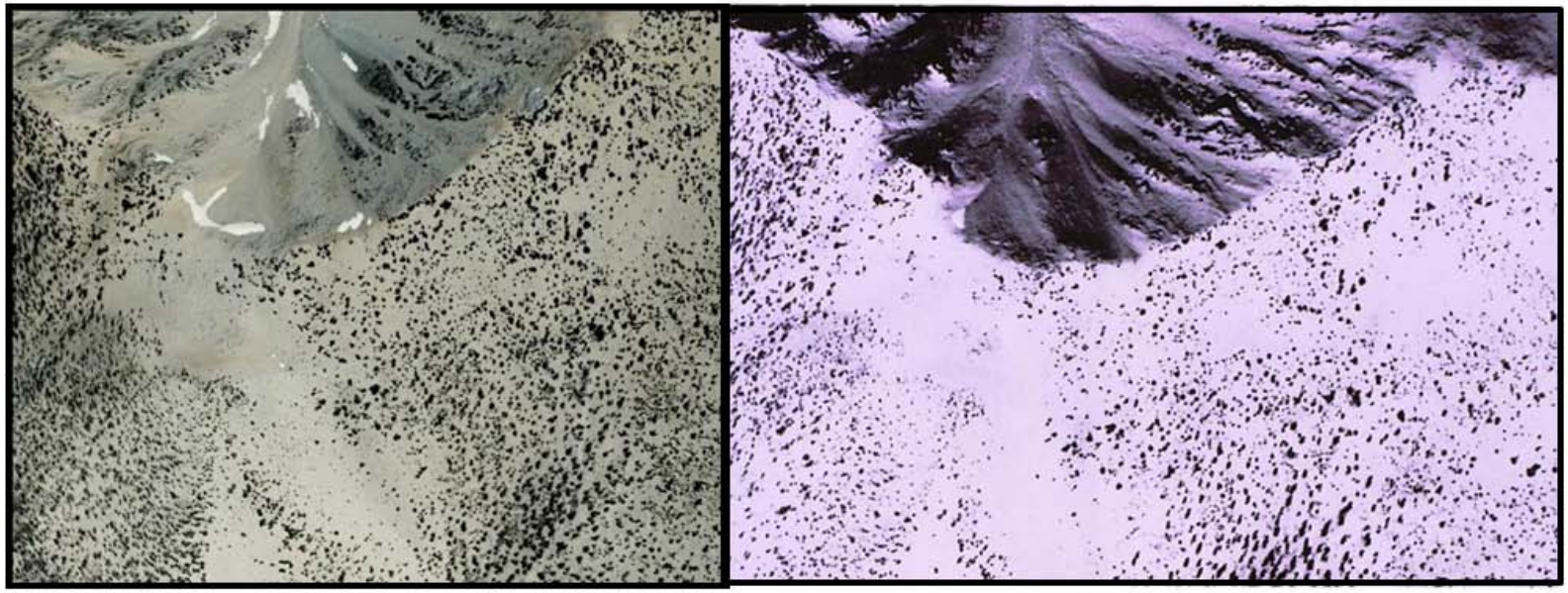

Figure 11: Aerial photographs of Mt. San Gorgonio in 2009 (left) and 1938 (right).

Table 3. Population data obtained from georeferenced aerial photographs in 1938 and 2009 on Mt. San Gorgonio.

	Site	Elev. (m)	Exposure	Total Trees 1938	Recruits	Mortalities	Total Trees 2011	Tree Cover % 1938	Tree Cover % 2011
San Gorgonio	SGR-L-1	3394	SE	2	0	2	0	1	0
	SGR-L-2	3334	SE	5	9	0	14	1	3
	SGR-L-3	3386	SE	0	0	0	0	0	0
	SGR-L-4	3391	SW	4	0	0	4	1	1
	SGR-W-1	3414	SW	17	5	0	22	8	10
	SGR-W-2	3383	SW	22	6	0	28	10	12
	SGR-W-3	3405	SW	21	3	1	23	6	6
	SGR-W-4	3356	S	37	4	2	39	13	13
	SGR-W-5	3329	SW	26	6	1	31	10	11
	SGR-W-6	3273	SW	30	6	1	35	12	12
	SGR-W-7	3379	SW	28	8	1	35	10	9
	SGR-W-8	3358	SW	22	2	2	22	9	10
	SGR-W-9	3400	SW	24	3	0	27	7	7
	SGR-W-10	3371	SW	26	3	0	29	6	6

Figure 12A : A close up of tree damage in 2011. Note the brown upper canopies.

Figure 12B: A Google map of photo locations of tree damage in 1972, and a polygon analysis of damage in 2011, in the same areas as the point localities.

DISCUSSION

Mountain tree lines, the elevational limit of woody vegetation, are ultimately governed by temperature and photosynthetic carbon gain (Tranquillini 1979; Grace et al 2002). This limit is seen at Mt. San Gorgonio where trees have decreasing tree stature to dbh ratios with elevation, especially > 3000 m (Figure 6). LST increases in magnitude and spatial extent with elevation, corresponding with increasing wind speeds of the jet stream and frequency of foliar damage disturbances. The nonrandom local distribution of trees on the summit also represents a legacy of disturbances coupled with the jet stream such as excessive snowfall, LST, foliar injury, growing season snow cover, and stand-replacing wildfires. While mature forest collectively mitigates surface winds and snow accumulation heterogeneities, stand-denuding fires enlarge LST zones below the krummholz zone.

Mature subalpine forest grows to as high as 3000 m, with spatially homogenous snow accumulations, even in stand-replacement burns, as documented at JST in the wake of the San Bernardino Ridge. Forests consist of uniform, dense recruitment and growth of young trees, similar to subalpine forest successions in the California Sierra Nevada (Fites-Kaufman 2007). In a post-fire succession at JST, stems grew vertically from apical dominance to 10 m with limited flagging of branches, and had developed partial canopy closure after 142 years (Figure 7A). Diameter frequency distributions indicate that tree establishment was initially rapid, then slowed with increasing tree cover, as would be expected for shade-intolerant *Pinus contorta*. LST and recruitment gaps in

cornice zones were not evident in an earlier successional forest state on 1938 aerial photographs.

On exposed ridges and peaks, data at TFR and CHP show that the denudation of tall forest initiates LST in which tree successions on windward slopes is hindered by high winds and snow ablation, with tree densities of < 200 ha^{-1} are far below those at JST. Stems still exhibit vertical symmetry, with little flagging. Tree establishment on windward slopes preceded leeward establishment at both sites, the recolonization of leeward slopes was dependent on the development of plant growth and canopy roughness on windward slopes.

At TFR (Figure 7C) continuous stem recolonization is evidenced by variable dbh and tree stature, with a dbh cap of 40 cm representing the oldest trees establishing after the 1951 crown fire. The delay in lee slope recruitment is suggested by smaller dbh and stature of leeward than windward trees. Local leeward barrens persist in areas subject to late season snow drifts and cornices. Small dbh recruits suggest recent initial establishment into bare zones. The 1863 CHP burn has greater range in stem dbh distributions than at TFR (Figure 7B). Even so, tree stature is similar at both sites due to lower productivity rates at CHP than TFR. The windward slope of CHP was virtually barren on a 1900 ground photograph and on a 1938 aerial photograph (Figure 8). Windward tree densities of 150-170 stems ha^{-1} with forest cover of 20% are much less than JST which burned only six years later. A few 80 cm dbh individuals at CHP survived the 1863 fire as evidenced by basal fire scars. The lee slope is still barren

although small statured, low dbh stems had established contagiously into the bare zone since 1938. Newly colonized areas lie along the windward edge of the cornice zone. A cornice on October 1938 aerial photographs was proportionately larger than snow fields elsewhere compared to recent perennial snow years (compare Figures 3 and 8). Since interannual late snow distributions are fixed, we suggest that an increase windward forest cover and tree stature had reduced cornice development, allowing for incipient colonization of the lee slope over the past 70 years.

The small area of stand-replaced forests in the region since 1863 is evidence that current rates of burning is unlikely to change broad-scale tree lines over long time scales. In California subalpine forest, fire intervals occur at scales of centuries in subalpine forest as a manifestation of stand-replacement fire cycles. The absence of surviving tree cover after fires precludes recurrences until there is establishment and maturation of an entirely new forest (reviews in Fites Kaufman 2007; Minnich 2007). In addition, drought levels sufficient for burning occurs rarely, regardless of the successional status and cumulative fuel build up. Subalpine forest has deep snow most years, and terminal melt in early summer is soon followed by thundershowers of the North American monsoon (Stenstrud et al. 1997). The JST (1869), CHP (1863), and TFR (1951) burns, as well as other burns in the region (1887, 1899 and 1913; Leiberg 1899, 1900; Minnich 1988) all occurred in extreme drought when PON < 50%, or the last winter storms ceased prematurely (e.g., January or February; Figure 4). Abnormally early terminal spring snow melt was followed by high fire hazard until the arrival of early summer thunderstorms, or later if monsoon rains fail. Most stand replacement burns occur in June or July. Indeed, we

cannot preclude the unlikely possibility that krummholz on SGR is a manifestation of a post-fire succession but previous fire history is undocumented. High mountain summits such as nearby Mt. San Jacinto (elev., 3300 m) experience numerous single tree fires from lightning, but these seldom kill trees, and flame line burns are unknown (Shepherd and Lassoie 1998).

At SGR > 3200 m krummholz forest on windward slopes, trees sustain chronic canopy wind shear injury that maintains stands in an "early successional" state and continuous LST. The northeastward long axes of krummholz stems suggest that windward foliar shear disturbances observed in 1971-72 and on Google Earth in 2010 **(**Figure 11) is the fundamental long-term process that shapes krummholz morphology. The mean storm snow line in southern California is 2200 m with summit temperatures, assuming moist adiabatic lapse rates, ranging from -5 to -10° C at moist adiabatic lapse rates, allowing for only limited snow and ice accumulations in tree canopy. In both foliar injury episodes, the preceding winters had at least one intense subtropical frontal storm characterized by snow lines approaching the highest peaks at 3000 m (700 mbar) recorded in National Weather Service radiosonde data at San Diego (December 1971, December 2009; Minnich 1986). With summit storm temperatures near 0º C, we hypothesize that windward tree canopies accumulated high density bulk ice derived from condensation of supercooled water vapor and liquid cloud droplets in cloud that subsequently froze in tree canopy, bypassing sublimation hoar frost of colder storms. Heavily iced branches were broken in high winds. Bulk ice advection is consistent with the focus of damage on windward and exterior crown faces of krummholz stems, as well

as tree shape. Hoar frost by sublimation of supercooled cloud vapor may contribute to canopy dieback, but produce less foliar accumulations (lower density solid precipitate) than bulk ice. Stem dieback is proportional to leader emergence above the canopy line. Windward canopy shelters leeward canopy from high winds, the recurrence of icing disturbances over long time scales "stretching" trees downwind (Figure 13).

The frequency of wind-ice injury disturbances is not documented by field studies. We estimate the frequency of such events using radiosonde data (Minnich 1986). Storm snow lines ≥ 3,000 m with precipitation > 5 cm 12 hr^{-1} are rare in the climate, with events for the period 1956-80 occurring in 1956-57, 1958-59, 1965-66, 1966-67, 1968-69, 1970-71, 1971-72, and 1979-80 (Minnich 1986). At these frequencies, we conclude that canopy dieback from bulk icing at rates of 1-3 events $decade^{-1}$ can readily reverse net tree growth.

The severity of LST processes near SGR is suggested by the formation of "tree streets" parallel to storm winds (Figure 14). It appears that extreme habitat limits recruitment to the immediate wake of upwind trees exclusively which locally reducwind speed and trap snow.

An alternative process in foliar damage is freeze desiccation. Transpiration demand in abnormally hot winter days is coupled with snow-free frozen ground that limits water uptake, desiccating the foliage, first addressed by Aulitsky (1961) in the European Alps. However, freeze desiccation, would be expected to produce foliar damage to whole canopies, not just windward faces. In addition, winters in California are

mild and permafrost is unknown. Hence, roots have access to unfrozen soil water at any depth, even in exposed ridgelines subject to snow ablation. Weather balloon soundings at San Diego seldom record temperatures < -10° C and air mass freezing lines in winter are routinely >3000 m between storms (Minnich 1984).

Trees are also susceptible to extreme drought. The winter of 2002 was the driest year in southern California since instrumental records began in 1849 (Minnich 2007), but this climatic singularity produced trivial tree mortality on subalpine forest > 2800 m due apparently to low temperature and transpiration demand in the climate. The exceptional infrequency of drought mortality may contribute to millennial aged life spans in subalpine forest tree species, as documented in *Pinus flexilis* (e.g., Brown and Schoettle 2008; Millar et al 2007) and *Pinus longaeva* in the White Mountains of California (La Marche 1972, La Marche 1974).

Long tree longevity in SGR krummholz dbh distributions and georeference population turnover data from 1938 and 2009 aerial photographs. The dbh of SGR trees are comparable or exceed those at lower elevation sites, despite lower productivity rates at the very margin of the tree line. Slow growth and hard wood offers resistance to insect pathogens, and tree are not buried in deep snow due to LST, thus precluding late summer snow cover. Georeferenced 1938 and 2009 aerial photographs record virtually fixed nearest-neighbor distribution of stems across the mountain. Only 10% of stems extent in 2009 had recruited or perished over the past 71 years (Table 2). Current turnover rates give stem life spans in the order of millennia averaged for the whole population.

Recruitment rates exceed mortality and predict a doubling in stand densities in ca. 300 years. However, tree cover increased by only 7% since 1938, reflecting the wind-ice damage events that limit net tree growth, i.e., canopy gain is being reversed by frequent wind and ice crown damage events.

Leeward bare zones experience late season to perennial snow in fixed interannual distributions in complex terrain (Figures 2- 4). Terminal snowmelt on windward southwest-facing exposures precedes the ascent of the zonal snow line (Minnich 1984), a consequence of snow ablation. In the winter precipitation season, snow depths rise no higher than the local stature of krummholz. Krummholz burial produces smooth aerodynamic snow surfaces, increasing LST efficiency. It follows that LST increases with mean annual precipitation at climatic scales because tree burial spans a greater proportion of the winter precipitation season. Burial also becomes more spatially extensive with increasing precipitation. Snow that fails to accumulate on windward slopes is transported in blowing snow to leeward slopes as ridgeline cornices and leeward snow drift accumulations. LST is invoked as the primary mechanism in snow accumulation distribution because of predictable year to year snow deposition fields (Figure 3), as opposed to variable interannual snow melt distributions arising from slab avalanches.

Krummholz forest in snow ablation zones extend only to ridgelines that border barren leeward snow accumulation zones (Figure 5). Leeward slopes have remained barren since 1938 under frequent episodes of growing season and occasional perennial

snow cover. Newspaper records and photographs document perennial snow on leeward slope in 30% of years (Figure 3), despite a mean annual precipitation of only 90 cm (Minnich 1986). Since annual melt rates in California mountain watersheds far exceed mean snow water equivalent (SWC, e.g., Elder et al. 1991, Miller 1981), growing season perennial snow accumulations are dependent on LST on snowpack heterogeneity.

Estimates of snowpack water content required to survive a summer melt season, assuming daily melt rates of 1.0 cm day^{-1}, give SWC values of cornices and leeward LST accumulations that exceed homogeneous accumulations at nearby snow survey sites by a factor of two (Minnich 1984; Owen et al. 2003). The SWE of perennial accumulations exceed 300 cm. Moreover, snow accumulation heterogeneities may be intensified in above normal precipitation years due to (1) increasing precipitation duration i.e., more time in blowing snow; (2) higher 700 mbar wind speeds with precipitation intensities proportionate with the strength of the jet stream and vapor flux, and (3) decreasing canopy wind friction with snow burial of trees. With enhanced LST efficiencies snow fields produced in the wettest years, e.g., 1883-84, 1889-90, 1992-93 may persist several years to as long as a decade (Figures 3 and 5). In fact, data for precipitation at Los Angeles and perennial snow years suggest that permanent snowfields would form if mean annual precipitation increased by only 30% (Figure 4).

Tree injury on leeward slopes is characterized by bole and crown death except for survival of lowest branches. Wind shear damage is diminished compared to trees on windward slopes. Leeward slope mortality is common, and there has been negligible on

repeat aerial photographs since 1938 (Figure 12). Leeward snow drifts breach the growing season, and perennial snow directly kills trees due to reduced photosynthesis. Short life spans are evidenced by low tree stature and dbh, and scarcity of leeward stems (Figure 7D). Tree establishment in snow free periods may persist for a decade or longer in drought, e.g., 1896-1905, 1922-1935, 1942-1951, 1952-67, 1984-1992 (Figure 4), but recruitment is reversed by singular perennial snow events. Barrens are extensive on the headwalls and basins of glacial cirques. While these areas also receive heavy deposition from LST, tree colonization appears to be constrained by poor soil development on bedrock cliffs and boulder fields left by glaciers that disappeared as recently as the Younger Dryas (12.5 ka, Owen et al., 2003).

Climate and Global tree lines.

At global scales, the tree line is predicted to ascend mountain slopes with planetary warming because the upper elevational boundary of woody vegetation is assumed to represent temperature limitations to positive net photosynthesis (MacDonald et al, 1993; Dullinger et al, 2004). A central question is how photosynthesis is constrained by other physical processes that limit tree growth at global scales (Smith et al. 2003; Johnson et al. 2004). LST affects mountain tree lines throughout the temperate latitudes (30-50°) where climates with mild summers allow tree lines to extend upslope to elevations at the base of the polar front jet stream (Palmén and Newton 1965). Poleward of lat. 50°, lower tree lines phase with lighter circulations of lower tropospheric mixed layer, as evidenced by cirque orientations (Evans 2006; Mindrescu 2010). Equatorward

of 30° LST has limited importance because isotropic temperature fields of the tropics produce light winds through the troposphere.

In climate change, atmospheric temperature is hydrostatically linked to the geostrophic wind (Byers 1959: 211) which drives LST. Hence, any nonuniform spatial change in ambient temperatures at climatic scales will also produce novel change in jet stream configuration and local winds. At SGR, LST continues unabated due to chronic injury to windward krummholz trees by wind-driven processes, the paucity and low stature of tree cover permitting snow ablation, and downstream leeward slope snow accumulations that are lethal to tree establishment. Even with recent global warming, lee slope tree colonization has recently been inhibited by increased frequency of years in perennial snow (Figure 4**).** After only two perennial snow years between 1941 and 1968, a period of protracted drought in the southwestern US (e.g., Meko et al. 1995; Ni et al. 2002), there has been 11 events since 1969. In recent decades, southern California and the Southwest has experienced greater precipitation than in the mid-20th century due to high frequency of El Niño/Southern Oscillation events coupled with the negative phase Pacific Decadal Oscillation (Dettinger et al. 1998; Cayan 1996; McCabe and Dettinger 1999). Indeed, the 30-yr running mean annual precipitation at Los Angeles has increased from 33.1 cm in 1976 to 41.3 in 2005 (Figure 4). Fundamentally, global temperature does not directly reduce snow accumulations because melt is a consequence of solar and terrestrial radiant loading (Miller 1981); there have been no clear trends in SWE at high elevations even with predicted rises in storm snow lines (Bales et al. 2006). Predicted

carbon gains from increasing temperature have been accompanied by windward canopy damage and increasing lee slope snow burial.

As net primary productivity approaches zero with altitude, an essential issue in the growth of plant canopy is the separation of intrinsic productivity from physical dieback over ecological time scales. The question is what is carbon gain in canopy versus the rate of canopy removal due to wind-driven disturbances and snow burial over the life of the tree, that reduce photosynthetic capacities. Without mass loss from LST, we predict that a hypothetical increase in forest canopy would permit tree colonization to higher elevations than the modern empirical limit, i.e., the photosynthetic limit is higher than the empirical limit. The potential biomass gain without LST is bolstered by wind-pollination in *Pinus flexilis* and *P. contorta* which assures that krummholz represents phenotypic plasticity rather than ecotypic differentiation. While individual trees fixing suboptimal carbon have reduced crown strength against wind disturbances, dwarfed members near the tree line likely have the prevailing genotype of tall trees at lower elevations.

The understanding of modern steady-state tree line dynamics also requires the integration of climate change relationships with millennial life spans of subalpine species (e.g., *Pinus longaeva*; La Marche 1974). Long-established trees exploit large niche space, and have greater capacity to respond to climate variability than young stems (Davis 1981; Davis and Botkin 1985; Grulke et al. 2009). The resulting lag time between climate change and vegetation response in long-lived ecosystems, which is rarely

considered in vegetation modeling studies, has been documented in many ecosystems (Thompson 1990). At SGR, repeat aerial photographs since 1938 document limited demographic turnover, modest increase in stand density, and persistence in the tree line (Table 2). Tree lines have remained stable since the first aerial photograph coverage in 1938.

Figure 13: View south of the same krummholz trees. **A.** 1972. Recent foliar damage on windward (right side) faces of tree crowns and surviving canopy on leeward faces (far left). **B.** 1980 Ascending leader in leeward crown, with limited net growth of windward face. Dead stems from previous injury are seen in mid-canopy.

Figure 14: Tree “street” alignment parallel to storm winds on Mt. San Gorgonio.

CONCLUSION

Modeling simulations of future vegetation place at risk an incomplete understanding of environmental processes affecting tree limits. Simulations also leave an untested legacy of predictions that must await the arrival of predicted reference periods. Theory cannot advance as long as hypotheses remain untested empirically. This study shows that the tree line is affected by LST, foliar wind damage, growing season snow burial and wildfires, not just temperature change constraints on photosynthesis. These variables operate at different time scales that must be integrated for in the assessment of current tree lines. Moreover, the spatial variability of LST importance yields azonal fluctuations in tree line that needs to be accounted for in model predictions of tree lines. Future studies under the new global warming paradigm should focus on empirical change in global tree lines using time-series aerial photography and space imagery. A broadscale inventory of tree lines is now made possible with new online technologies such as Google Earth and available historical photography such as Earth Explorer (U.S. Geological Survey). Time-series maps of tree lines will refine our understanding of tree line dynamics and help constrain model predictions of forest change.

REFERENCES

Aulitzky, H.: 1961, Die Bodentemperaturen in der Kampfzone oberhalb der Waldgrenze und im subalpinen Zirben-Larchenwald. – Mitteilungen der Forstlichen Bundes-Versuchsanstalt Mariabrunn 59: 155-208.

Bales, R.C., N.P. Molotch, T.H. Painter, M.D. Dettinger. R. Rice, and J. Dozier. 2006. Mountain hydrology of the western United States. Water Resources Research 42: W08432.

Brown, P.W. and A.W. Schoettle. 2008. Fire and stand history in two limber pine (*Pinus flexilis*) and Rocky Mountain bristlecone pine (*Pinus aristata*) stands in Colorado. International Journal of Wildland Fire 17: 339-347.

Cayan, D.R. 1996. Interannual climatic variability and snowpack in the western United States. Journal of Climate 9:928-948.

Davis, M.B. and Botkin. 1985. Sensitivity of cool-temperate forests and their fossil pollen record to rapid temperature change. Quaternary Research 23: 327-340.

Davis, M.B. 1981. Quaternary history and stability of forest communities. Forest Succession: Concepts and application (D.C. West, H.H. Shugart, and D.B. Botkin, eds.). Springer-Verlag, New York: 132-153.

Dettinger, M.D., D.R. Cayan, H.F. Diaz and D.M. Meko. 1998. North-south precipitation patterns in western North America on Interannual-to-decadal timescales. Journal of Climate 11: 3095-3111.

Dullinger, S., Dirnbock, T., and Grabher, G.: 2004, Modelling climate change driven treeline shifts: relative effects of temperature increase, dispersal and invasibility. Ecology, 92: 241-252.

Elder, K. J. Dozier, and J. Michaelsen. 1991. Snow accumulation and distribution in an alpine watershed. Water Resources Reserarch 27, 1541-1552.

Evans, I.S. 2006. Local aspect asymmetry of mountain glaciation: A global survey of consistency of favoured directions for glacier numbers and altitude. Geomorphology 73: 166-184.

Fites-Kaufman, P. Rundel, N. Stephenson, and D.A. Weixelman. 2007. Montane and subalpine vegetation of the Sierra Nevada and Cascade Ranges. In, Terrestrial Vegetation of California, 3rd edition (M.G. Barbour, T. Keeler-Wolf, and A.A. Schoenherr, eds.), University of California Press. Berkeley: 456-493.

Grulke, N.E., R.A Minnich, T.D. Paine, S.J. Seybold, D.J Chavez, M.E. Fenn, P.J. Riggan and A. Dunn. 2009. Pp. 339-364 in: Wildland fires and air pollution.

Gilbert, G. K. 1904. Cirque asymmetry in the Sierra Nevada of California. The Journal of Geology 12: 579-588.

Grace J. F. Berninger, and L. Nagy 2002. Impacts of climate change on the tree line. Annals of Botany 90: 537-544.

Google Earth Imagery, 2007, 2009, 2011. San Gorgonio Wilderness.

Holtmeier, F.K., 2003, Mountain Timberlines; Ecology, Patchiness, and Dynamics. Kluwer Academic Publishers, 2003.

Johnson, D.M. M.J. Germino and W.K Smith. 2004. Abiotic factors limiting photosynthesis in *Abies lasiocarpa* and *Picea engelmannii* seedlings below and above the alpine timberline. Tree Phyiology 24: 377-386.

LaMarche, V.C.: 1974, Holocene climatic variations inferred from treeline fluctuations in the White Mountains, California. Quaternary Research 3, 632-60.

Lehning, M. H. Löwe, M. Ryser, and N. Raderschall. 2008. Inhomogeneous precipitation distribution and snow transport in steep terrain. Water Resources Research 44: W07404

MacDonald, G. M., Edwards, T. W. D., Moser K. A., Pienitz, R., and Smol, J. P.: 1993, Rapid response of treeline vegetation and lakes to past climate warming. Nature, 361: 243-246.

McCabe, G.J. an M.D. Dettinger. 1999. Decadal variations in the strength of ENSO connections with precipitation in the western United States. International Journal o Climatology 19:1399-1410.

Meko, D. C.,W. Stockton, and W.R. Boggess. 1995. The tree-ring record of severe sustained drought. 2007. Journal of the American Water Resources Association. 31: 789-801.

Millar, E.I. R.D. Westfall, and D.L. Delany. 2007. Rersponse of high-elevation limber pine (Pinus flexilis) to multiyear droughts and 20th-century warming, Sierra Nevada, California, USA. Canadian Journal of Forest Research 37:2508-2520

Miller, D.H. 1981. Energy at the surface of the Earth: An introduction to the energetics of ecosystems. International Geophysics Series Volume 27. pp. 517.

Mindrescu, Evans and Cox Journal of Quaternary Science. 2010. Climatic implications of cirque distribution in the Romania Carpathians: Paleo wind directions during glacial periods.

Minnich, R. A., 1984: Snow Drifting and Timberline Dynamics on Mount San Gorgonio, California, U.S.A. Arctic and Alpine Research, Vol. 16, No. 4, 1984, pp. 395-412.

Minnich, R. A. 1988. The biogeography of fire in the San Bernardino Mountains of California: A historical survey. University of California Publications in Geography 28:1-120.

Minnich, R. A., 1986: Snow Levels and Amounts in the Mountains of Southern California. Journal of Hydrology, 89: 37-58.Minnich, R. A.: 2006, California climate, paleoclimate and paleovegetation. In, Terrestrial vegetation of California, 3rd edition (M.G. Barbour, T. Keeler-Wolf, and A.S. Schoenherr, eds.). University of California Press, Chapter 2. (publication date, spring, 2007)

Minnich, R.A. 2007. Climate, paleoclimate and paleovegetation. In, Terrestrial Vegetation of California, 3rd edition (M.G. Barbour, T. Keeler-Wolf, and A.A. Schoenherr, eds.), p. 43-70. University of California Press. Berkeley.

Minnich, R.A. 2008. California's fading wildflowers: Lost legacy and biological invasions. University of California Press.

Morton, D.M., Cox, B.F., and Matti, J.C.: 1980, Geological map of the San Gorgonio Wilderness, San Berardino County, California: U.S. Geological Survey, Miscellaneous Field Studies Map MF-1161-A, scale 1:62500.

National Aeronautics and Space Administration, Goddard Institute for Space Studies.: http://data.giss.nasa.gov/gistemp/.

National Oceanographic and Atmospheric Administration, National Climatic Data Center.: http://www.ncdc.noaa.gov.

National Oceanographic and Atmospheric Administration, National Weather Service. Downtown Los Angeles Climate Page; 1877-2005 data: http://www.wrh.noaa.gov.

Ni, F. T. Cavazos, M.K. Hughes, A.C. Comrie, and G. Funkhouser. 2002. Cool-season precipitation in the southwestern USA since AD 1000: comparison of linear and nonlinear techniques for reconstruction. International Journal of Climatology 22: 1645-1622.

Owen, L. A., Finke, Minnich, R. A, and Perez, A. E., 2003: Extreme southwestern margin of late quaternary glaciation in North America: Timing and controls. Geological Society of America, v. 31; no. 8; p. 729-732.

SCAMP (Southern California Area Mapping Project, San Gorgonio Quadrangle). US. Geological Survey, California Geological Survey. http://geomaps.wr.usgs.gov/archive/scamp/html/scamp.html

Scuderi, L.A.: 1987, Late-Holocene upper timberline variation in the southern Sierra Nevada. Nature 325: 242-244.

Sheppard, P.R., and J.P. Lassoie. 1998. Fire regime of the lodgepole pine forest of Mt. San Jacinto, California. Madrono 45: 47-56.

Smith, W.K, M.J. Germino, T.E. Hancock and D.M. Johnson. 2003. Another perspective on altitudinal limits of alpine timberlines. Tree Physiology 23: 1101-1112.

Stensrud, D.J. R.L. Gall, and M.K. Nordquist. 1997. Surges over the Gulf of Californnia during the Mexican monsoon. Monthly Weather Review 125: 417-437.

Thompson, R.S. 1990. Late Quaternary vegetation and climate in the Great Basin. pp. 200-239 In: Packrat Middens: The last 40,000 yhears of biotic change (J.L. Betancourt, T.R. Van Devender, and P.S. Martin, eds.). University of Arizona Press.

Tranquilini, W.: 1979, Physiological Ecology of the Alpine Timberline, Tree Existence at High Altitudes with Special Reference to the European Alps. Springer-Verlag, Berlin, Heidelberg, New York, 1979.

United States Forest Service: Index of Species Information; Pinus contorta variation Murrayana. www.fs.fed.us/database/feis/plants/tree/pinconm/all.html.

Watanabe, T. 1988. Studies of snow accumulation and ablation on perennial snow patches in the mountains of Japan. Teiji Watanabe Progress in Physical Geography 1988 Vol 12. 560.

Appendix 1:Site and Quadrat Data Table

	Location	TTFR Q1	TTFR Q2	TTFR Q3	TTFR Q4	TTFR Total	CP Q1	CP Q2	CP Q3	CP Q4	CP Total	SG Q1	SG Q2	SG Q3	SG Q4	SG Total	JS Total
Quadrat	Bearing (in ˚T)	225	240	256	255	244	238	233	228	237	234	264	235	255	225	245	238
	Start Elevation (m)	2999	2993	2985	3053	3007.5	3251	3232	3201	3187	3217.8	3324	3371	3407	3418	3380	3045
	Slope	28.0%	16.7%	42.4%	32.9%	30.0%	36.7%	29.3%	32.9%	27.7%	31.6%	17.4%	32.6%	35.7%	20.8%	26.6%	26.7%
	Total Trees	99	72	284	121	576	67	187	140	208	602	110	142	75	69	396	471
	Tree Density (tph)	261	181	753	314	374	352	478	359	537	515	278	374	203	174	257	1216
Tree Demographics	P. contorta	21	28	11	20	80	55	179	121	146	501	26	16	4	11	57	453
	P. flexilis	36	29	231	79	375	12	8	19	62	101	84	126	71	58	339	18
	P. jeffreyi	39	15	42	22	118	0	0	0	0	0	0	0	0	0	0	0
	J. Occident	3	1	0	0	4	0	0	0	0	0	0	0	0	0	0	0
	0-1m	51	30	177	79	337	4	22	15	52	93	30	44	11	21	106	18
	1-2m	19	18	38	19	94	6	35	12	32	85	67	75	40	40	222	50
	2-3m	5	9	24	6	44	2	38	12	19	71	12	23	18	8	61	100
	3-4m	4	4	16	11	35	2	21	14	17	54	1	0	5	0	6	70
	4-5m	8	1	7	4	20	6	9	6	20	41	0	0	1	0	1	42
	5m+	12	10	14	2	38	47	62	81	68	258	0	0	0	0	0	42
	0-5cm	55	35	199	79	368	3	15	11	48	77	29	23	7	16	75	83
	5-10cm	16	19	44	17	96	9	35	16	37	97	34	24	11	17	86	93
	10-15cm	7	6	22	13	48	3	37	13	25	78	21	33	11	18	83	95
	15-20cm	4	5	8	5	22	2	29	19	31	81	19	27	13	3	62	88
	20-25cm	2	2	5	4	13	5	16	12	28	61	3	18	7	4	32	62
	25cm+	15	5	6	3	29	42	54	62	34	192	3	14	25	7	49	51

Appendix 2. Annual precipitation, and running averages at 3 yr, 5 yr, 10 yr and 30 yr at Los Angeles Downtown, and years with perennial snow reported in newspapers

Precipitation Season (Jul 1-Jun 30)	Perennial snow (x)	Precipitation (inches)	3yr-mean	5yr-mean	10-yr mean	30 yr mean
1878	x	21.26				
1879		11.35				
1880	x	20.34	17.65			
1881		13.13	14.94			
1882		10.40	14.62	15.30		
1883		12.16	11.90	13.48		
1884	x	38.18	22.03	18.84		
1885	x	9.21	19.85	16.62		
1886	x	22.31	23.02	18.45		
1887	x	14.05	15.19	19.18	17.24	
1888	x	13.87	16.74	19.52	16.50	
1889	x	19.28	15.73	15.74	17.29	
1890	x	34.84	22.66	20.87	18.74	
1891	x	18.36	24.16	20.08	19.27	
1892	x	11.85	21.68	19.64	19.41	
1893	x	26.28	18.83	22.12	20.82	
1894		6.73	14.95	19.61	17.67	
1895	x	16.11	16.37	15.87	18.68	
1896		8.51	10.45	13.87	16.99	
1897		18.83	14.48	15.29	17.47	
1898		7.06	11.47	11.45	16.79	
1899		5.59	10.49	11.22	15.42	
1900		7.91	6.85	9.58	12.72	
1901		16.29	9.93	11.14	12.52	
1902		10.60	11.60	9.49	12.39	
1903		19.32	15.40	11.94	11.70	
1904		8.72	12.88	12.57	11.94	
1905	x	19.52	15.82	14.89	12.24	
1906	x	18.65	15.63	15.36	13.25	0.00
1907	x	19.30	19.16	17.10	13.30	16.39
1908		11.72	16.56	15.58	13.76	16.32
1909	x	19.18	16.73	17.67	15.12	15.94
1910		12.63	14.51	16.28	15.59	15.69
1911	x	16.18	16.00	15.80	15.58	15.79
1912		11.60	13.47	14.26	15.68	16.17
1913		13.42	13.73	14.60	15.09	16.28
1914	x	23.65	16.22	15.50	16.59	15.87
1915	x	17.05	18.04	16.38	16.34	15.65
1916	x	19.92	20.21	17.13	16.47	15.57

1917		15.26	17.41	17.86	16.06	15.61
1918		13.86	16.35	17.95	16.28	15.61
1919		8.58	12.57	17.44	15.22	15.25
1920		12.52	11.65	14.03	15.20	14.51
1921		13.65	11.58	12.77	14.95	14.35
1922	x	19.66	15.28	13.65	15.76	14.61
1923		9.59	14.30	12.80	15.37	14.05
1924		6.67	11.97	12.42	13.68	14.05
1925		7.94	8.07	11.50	12.77	13.78
1926		17.56	10.72	12.28	12.53	14.08
1927		18.03	14.51	11.96	12.81	14.05
1928		9.77	15.12	11.99	12.40	14.14
1929		12.66	13.49	13.99	12.81	14.38
1930		11.52	11.32	13.91	12.71	14.50
1931		12.52	12.23	12.90	12.59	14.38
1932		16.93	13.66	12.68	12.32	14.59
1933		11.88	13.78	13.10	12.55	14.34
1934		14.94	14.58	13.56	13.38	14.54
1935	x	21.66	16.16	15.59	14.72	14.60
1936	x	13.47	16.69	15.78	14.35	14.44
1937	x	22.41	19.18	16.87	14.78	14.55
1938	x	23.43	19.77	19.18	16.14	14.94
1939		13.07	19.64	18.81	16.18	14.73
1940		19.21	18.57	18.32	16.95	14.95
1941	x	31.26	21.18	21.88	18.83	15.46
1942		11.18	20.55	19.63	18.26	15.44
1943		18.17	20.20	18.58	18.88	15.60
1944		19.22	16.19	19.81	19.31	15.45
1945		11.59	16.33	18.28	18.30	15.27
1946		11.65	14.15	14.36	18.12	15.00
1947		12.36	11.87	14.60	17.11	14.90
1948		7.22	10.41	12.41	15.49	14.68
1949		7.99	9.19	10.16	14.99	14.66
1950		10.59	8.60	9.96	14.12	14.59
1951		8.21	8.93	9.37	11.82	14.41
1952	x	26.21	15.00	12.04	13.32	14.63
1953		9.46	14.63	12.49	12.55	14.63
1954		11.99	15.89	13.29	11.73	14.80
1955		11.94	11.13	13.56	11.76	14.94
1956		16.00	13.31	15.12	12.20	14.88
1957		9.54	12.49	11.79	11.92	14.60
1958		21.13	15.56	14.12	13.31	14.98
1959		5.58	12.08	12.84	13.07	14.74
1960		8.18	11.63	12.09	12.82	14.63
1961		4.85	6.20	9.86	12.49	14.38

1962		18.79	10.61	11.71	11.75	14.44
1963		8.38	10.67	9.16	11.64	14.32
1964		7.93	11.70	9.63	11.23	14.09
1965		13.68	10.00	10.73	11.41	13.82
1966		20.44	14.02	13.84	11.85	14.06
1967	x	22.00	18.71	14.49	13.10	14.04
1968		16.58	19.67	16.13	12.64	13.81
1969	x	27.47	22.02	20.03	14.83	14.29
1970		7.74	17.26	18.85	14.79	13.91
1971		12.32	15.84	17.22	15.53	13.28
1972		7.17	9.08	14.26	14.37	13.15
1973		21.26	13.58	15.19	15.66	13.25
1974		14.92	14.45	12.68	16.36	13.11
1975		14.35	16.84	14.00	16.43	13.20
1976		7.21	12.16	12.98	15.10	13.05
1977		12.30	11.29	14.01	14.13	13.05
1978	x	33.44	17.65	16.44	15.82	13.92
1979	x	19.67	21.80	17.39	15.04	14.31
1980	x	26.98	26.70	19.92	16.96	14.86
1981		8.96	18.54	20.27	16.63	14.88
1982		10.71	15.55	19.95	16.98	14.37
1983	x	31.28	16.98	19.52	17.98	15.09
1984		10.43	17.47	17.67	17.53	15.04
1985		12.82	18.18	14.84	17.38	15.07
1986		17.86	13.70	16.62	18.45	15.13
1987		7.66	12.78	16.01	17.98	15.07
1988		12.48	12.67	12.25	15.89	14.78
1989		8.08	9.41	11.78	14.73	14.86
1990		7.35	9.30	10.69	12.76	14.84
1991		11.99	9.14	9.49	13.07	15.08
1992		21.00	13.45	12.18	14.10	15.15
1993	x	27.36	20.12	15.16	13.70	15.78
1994	x	8.11	18.82	15.16	13.47	15.79
1995	x	24.35	19.94	18.56	14.62	16.14
1996		12.44	14.97	18.65	14.08	15.88
1997		12.40	16.40	16.93	14.56	15.56
1998	x	31.01	18.62	17.66	16.41	16.04
1999		9.09	17.50	17.86	16.51	15.42
2000		11.57	17.22	15.30	16.93	15.55
2001		17.94	12.87	16.40	17.53	15.74
2002		4.42	11.31	14.81	15.86	15.65
2003		16.42	12.93	11.89	14.78	15.49
2004		9.25	10.03	11.92	14.89	15.30
2005	x	37.96	21.21	17.20	16.26	16.08
2006		13.19	20.13	16.25	16.33	16.28
2007		3.21	18.12	16.01	15.41	15.98

2008		13.53	9.98	15.43	13.66	15.32
2009		9.08	8.61	15.39	13.66	14.96
2010		16.36	12.99	11.07	14.14	14.61
2011	x	20.20	15.21	12.48	14.36	14.99